© 2021. Published by The Company of Biologists Ltd | Development (2021) 148, dev195222. doi:10.1242/dev.195222

RESEARCH ARTICLE

Arc1 and the microbiota together modulate growth and metabolic traits in *Drosophila*

Scott A. Keith, Cassandra Bishop, Samantha Fallacaro and Brooke M. McCartney*

ABSTRACT

Perturbations to animal-associated microbial communities (the microbiota) have deleterious effects on various aspects of host fitness, but the molecular processes underlying these impacts are poorly understood. Here, we identify a connection between the microbiota and the neuronal factor Arc1 that affects growth and metabolism in *Drosophila*. We find that *Arc1* exhibits tissue-specific microbiota-dependent expression changes, and that germ-free flies bearing a null mutation of *Arc1* exhibit delayed and stunted larval growth, along with a variety of molecular, cellular and organismal traits indicative of metabolic dysregulation. Remarkably, we show that the majority of these phenotypes can be fully suppressed by mono-association with a single *Acetobacter* sp. isolate, through mechanisms involving both bacterial diet modification and live bacteria. Additionally, we provide evidence that Arc1 function in key neuroendocrine cells of the larval brain modulates growth and metabolic homeostasis under germ-free conditions. Our results reveal a role for Arc1 in modulating physiological responses to the microbial environment, and highlight how host-microbe interactions can profoundly impact the phenotypic consequences of genetic mutations in an animal host.

KEY WORDS: Growth regulation, Microbiota, *Acetobacter*, Arc1, Insulin signaling, Metabolism

INTRODUCTION

The physiology and life history traits of animals are shaped in remarkable ways by interactions with beneficial microorganisms (the microbiota). For many metazoans, microbial symbionts play integral roles in post-embryonic development and physiology to yield fit and fertile adults (McFall-Ngai et al., 2013; Robertson et al., 2019). Thus, perturbations to the microbiota can profoundly disrupt these processes. For example, germ-free (GF; microbiologically sterile) or antibiotic-treated mice exhibit decreased body fat (Smith et al., 2007), abnormal intestinal epithelial architecture (Hayes et al., 2018) and neurodevelopmental defects (Sampson and Mazmanian, 2015). In humans, gut bacterial dysbiosis has been implicated in the pathogenesis of type 2 diabetes (Larsen et al., 2010), obesity (Shen et al., 2013), autism (Gilbert et al., 2013) and other disorders. However, the molecular factors that actuate microbial influence on host physiology and development are incompletely understood. *Drosophila melanogaster* and its gut microbiota are an ideal model to discover such factors, given *Drosophila*'s extensive genetic resources and the technical ease of generating GF and gnotobiotic flies (Broderick and Lemaitre, 2012; Douglas, 2018).

From a screen to identify microbiota-responsive genes, we discovered altered levels of *Drosophila Activity-regulated cytoskeleton associated protein 1* (*Arc1*) transcript in GF flies. *Arc1* is a *Drosophila* homolog of mammalian *Arc* (also known as *Arg3.1*), a master regulator of synaptic plasticity in the brain (Carmichael and Henley, 2018; Shepherd and Bear, 2011). *Arc* transcription is highly upregulated during the encoding of novel information into neural circuits (Chen et al., 2020; Guzowski et al., 1999). Accordingly, reduced *Arc* expression impairs learning in rodents (Guzowski et al., 2000; Shandilya and Gautam, 2020), and defects in human ARC have been linked to neurological and neurodevelopmental disorders, including Alzheimer's disease (Bi et al., 2018), autism spectrum disorders (Alhowikan, 2016) and schizophrenia (Fromer et al., 2014). Both mammalian *Arc* and fly *Arc1* encode retroviral group-specific antigen-like amino acid sequences, and are predicted to have evolved independently from ancient Ty3/Gypsy retrotransposons (Ashley et al., 2018; Campillos et al., 2006; Cottee et al., 2019; Pastuzyn et al., 2018). Recently, it was shown that Arc/Arc1 can self-assemble into capsid-like structures that package and transport mRNAs into cultured neuronal cell lines and across synapses *in vivo*, constituting a previously unknown mechanism of cell-cell communication (Ashley et al., 2018; Erlendsson et al., 2019; Pastuzyn et al., 2018).

As with mammalian *Arc*, synaptic activity leads to strong transcriptional upregulation of fly *Arc1* (Guan et al., 2005; Mattaliano et al., 2007; Montana and Littleton, 2006; Mosher et al., 2015). At the larval neuromuscular junction (NMJ), synapse maturation and plasticity require Arc1 protein capsid-mediated transfer of *Arc1* mRNA from motoneuronal boutons to post-synaptic myocytes (Ashley et al., 2018). Further, *Arc1* loss-of-function mutants differentially express a repertoire of enzymes involved in central carbon metabolism, have altered metabolomic profiles, elevated fat levels, and are starvation resistant (Mattaliano et al., 2007; Mosher et al., 2015), suggesting that Arc1 controls metabolic homeostasis via unknown mechanisms.

In *Drosophila*, energy metabolism impacts developmental timing and whole-organism growth during the larval stages (Edgar, 2006). Developmental growth is diet dependent and genetically regulated by multiple nutrient-responsive, inter-organ signaling systems, including (but not limited to) the insect-specific steroid hormone 20-hydroxyecdysone (20E; Buhler et al., 2018; McBrayer et al., 2007) and the functionally conserved insulin/insulin-like growth factor (IIS) pathway (Brogiolo et al., 2001; Rulifson et al., 2002; Edgar, 2006). As in mammals, the *Drosophila* microbiota plays a crucial role in dietary influence on metabolic and developmental processes. Certain taxa of commensal bacteria (*Lactobacillus* and *Acetobacter* spp.) promote metabolic homeostasis and growth through mechanisms including nutritional provisioning and

Department of Biological Sciences, Carnegie Mellon University, Pittsburgh, PA 15213, USA.

*Author for correspondence (bmccartney@cmu.edu)

B.M.M., 0000-0002-5071-8550

Handling Editor: Irene Miguel-Aliaga
Received 21 July 2020; Accepted 1 July 2021

Development (2021) 148, dev195222. doi:10.1242/dev.195222

promoting host signaling pathways such as IIS (Chaston et al., 2014; Consuegra et al., 2020; Kamareddine et al., 2018; Keebaugh et al., 2018; Matos et al., 2017; Sannino et al., 2018; Shin et al., 2011). Interestingly, the microbiota can also reduce the severity of nutritional and developmental phenotypes resulting from host genetic mutations (Dobson et al., 2015; Ma et al., 2019). Although connections between the microbiota, host metabolism, and diet are widespread, an understanding of the molecular mechanisms that drive these connections is lacking.

Here, we uncover an interaction among Arc1, the microbiota and the host diet that impacts growth and metabolic traits in *Drosophila*. We show that *Arc1* transcript and protein levels change in tissue-specific patterns in GF flies, and loss of *Arc1* dramatically exacerbates the developmental growth delay of GF larvae. Furthermore, we found that a single *Acetobacter* isolate is sufficient to restore normal larval development and other hallmarks of metabolic health to *Arc1* mutants, partly through a mechanism that involves conditioning the larval diet. Selective *Arc1* expression in growth-regulating neuroendocrine cells suppresses the metabolic and developmental defects of GF *Arc1* mutants. Lastly, we provide evidence of both microbiota-dependent and -independent IIS and 20E dysregulation in *Arc1* null larvae. Together, our data reveal an experimental system wherein a single microbiota member supports the health of a metabolically destabilized host, and demonstrates a previously unknown role for Arc1 in mediating the animal's response to its microbial environment.

RESULTS

Arc1 transcript and protein are sensitive to microbial condition

To identify microbiota-responsive neuronal factors, we previously conducted a transcriptomic screen to identify *Drosophila* genes that are differentially expressed in GF adult heads. *Arc1* was among the genes most responsive to host microbial condition (Keith et al., 2019 preprint). Specifically, *Arc1* transcripts were elevated in the heads of adult wild-type *Drosophila* grown GF compared with flies grown in gnotobiotic (GNO) poly-association with a four-species bacterial community of two *Acetobacter* (*Acetobacter* sp., *A. pasteurianus*) and two *Lactobacillus* (*L. brevis*, *L. plantarum*) isolates (Fig. 1A). *Arc1* was previously identified in published RNA-seq comparisons of microbiota-associated versus GF adult guts (Bost et al., 2017; Dobson et al., 2016; Guo et al., 2014; Petkau et al., 2017). Consistent with these reports, and in contrast to the adult head, we found that *Arc1* transcripts are decreased in the adult gut following microbiota removal (Fig. 1A). These microbiota-dependent transcript changes occur in multiple wild-type lines, but both changes were not observed in every line (Fig. 1A).

Differential transcript abundances between microbiota-associated and GF animals could be a primary consequence of microbial loss, or may be secondary to metabolic changes resulting from sterile rearing. To test this, we measured *Arc1* levels in heads and guts of adult flies following starvation, which alters metabolic function (Wat et al., 2020; Zinke et al., 2002). Interestingly, *Arc1* mRNA decreased ∼50% in the heads of flies starved for 24 h, but was unchanged in starved guts (Fig. 1B), suggesting that *Arc1* expression may be sensitive to nutritional inputs as well as the microbiota.

Prompted by our transcript-level findings, we examined Arc1 protein in the adult brain and gut under GNO and GF conditions. Our analysis of the brain revealed a complex, cell type-specific effect of microbial condition. On the posterior brain surface, there was a significant increase in Arc1-positive cells (Fig. 1C,D). Although the level of Arc1 in the posterior central brain neurons was unaffected, Arc1 levels were decreased in GF animals in a neighboring cell type with distinct morphology (Fig. S1A,A″,C,D). By contrast, on the anterior brain surface, antennal lobe Arc1 expression was increased in GF animals (Fig. S1B,E). *Arc1* transcript is reported to be highly enriched in the adult midgut (FlyAtlas; Leader et al., 2018), but its immunostaining pattern has not been reported. We found that Arc1 was broadly expressed throughout the foregut and midgut in GNO animals, with greatly reduced expression in the hindgut (Fig. 1E). Consistent with *Arc1* mRNA (Fig. 1A), Arc1 protein in midgut cells was decreased ∼68% in GF animals (Fig. 1F).

Together, these results show that Arc1 transcript and protein levels change in complex, tissue- and cell type-specific ways in response to microbiota and nutritional deprivation.

Loss of the microbiota slows larval growth in *Arc1* mutants and a single *Acetobacter* species is sufficient to restore normal growth rate

Arc1 regulates lipid homeostasis and central carbon metabolite levels in *Drosophila* larvae (Mosher et al., 2015), and loss of *Arc1* results in enhanced adult starvation resistance (Mattaliano et al., 2007). These and other metabolic traits are also impacted by the microbiota, depending on dietary conditions and host genetic background (Dobson et al., 2015; Gnainsky et al., 2021; Judd et al., 2018; Yamauchi et al., 2020). One major consequence of GF-induced metabolic dysregulation in *Drosophila* is prolonged larval growth (Strigini and Leulier, 2016). To test for an interaction between the microbiota and *Arc1*, we raised wild-type flies (w^{1118}) and an *Arc1* deletion mutant ($Arc1^{E8}$; Ashley et al., 2018) from embryo to adulthood either GF or GNO, and monitored larval growth rate. Consistent with many previous reports (reviewed by Strigini and Leulier, 2016), GNO wild-type animals completed larval development significantly faster than their GF siblings (∼7.3 days versus ∼8.8 days, respectively; Fig. 2A, Table S1). Strikingly, the GF larval growth delay was dramatically extended in larvae lacking *Arc1*. Whereas GNO $Arc1^{E8}$ mutant larvae developed at a rate indistinguishable from GNO wild type, GF $Arc1^{E8}$ animals took on average ∼12.8 days to pupariate (Fig. 2A). These differences in larval growth rate were reflected in the rate of adult emergence (Fig. S2A). We observed a similar, though less protracted, developmental delay for two independently generated *Arc1* loss-of-function alleles ($Arc1^{esm18}$ and $Arc1^{esm113}$; Mattaliano et al., 2007) reared GF (Fig. S2B,C), and in GF $Arc1^{E8}/Arc1^{esm113}$ transheterozygotes (Fig. 2B). All larvae bearing deletions of *Arc1* developed at the wild-type rate when grown with the GNO bacterial community. *Arc2* is another *Drosophila* Arc homolog in a genomic locus adjacent to *Arc1*; the two proteins likely represent an ancestral duplication event (Pastuzyn et al., 2018). In contrast to *Arc1* depletion, a P-element insertion in the *Arc2* 3′ UTR, which decreased *Arc2* expression (Fig. S2D), had no effect on the developmental rate of GF larvae (Fig. S2E).

The microbiota-dependent growth delay of *Arc1* mutants motivated us to examine *Arc1* expression in the larval brain and gut under GNO and GF conditions. *Arc1* transcripts were decreased slightly but significantly in the brains of GF compared with GNO larvae, but were unaffected in the larval gut (Fig. 2C). In the larval brain, there were multiple clusters of Arc1-positive neurons and other Arc1-positive cells in the central brain lobes (Fig. 2D, Fig. S3), as previously reported (Mattaliano et al., 2007; Mosher et al., 2015). In contrast to transcript levels, the number of Arc1-positive cells in the central brain lobes was increased in GF animals (Fig. 2E, Fig. S3).

We next investigated whether the polymicrobial GNO community's ability to promote *Arc1* mutant growth rate was due

Development (2021) 148, dev195222. doi:10.1242/dev.195222

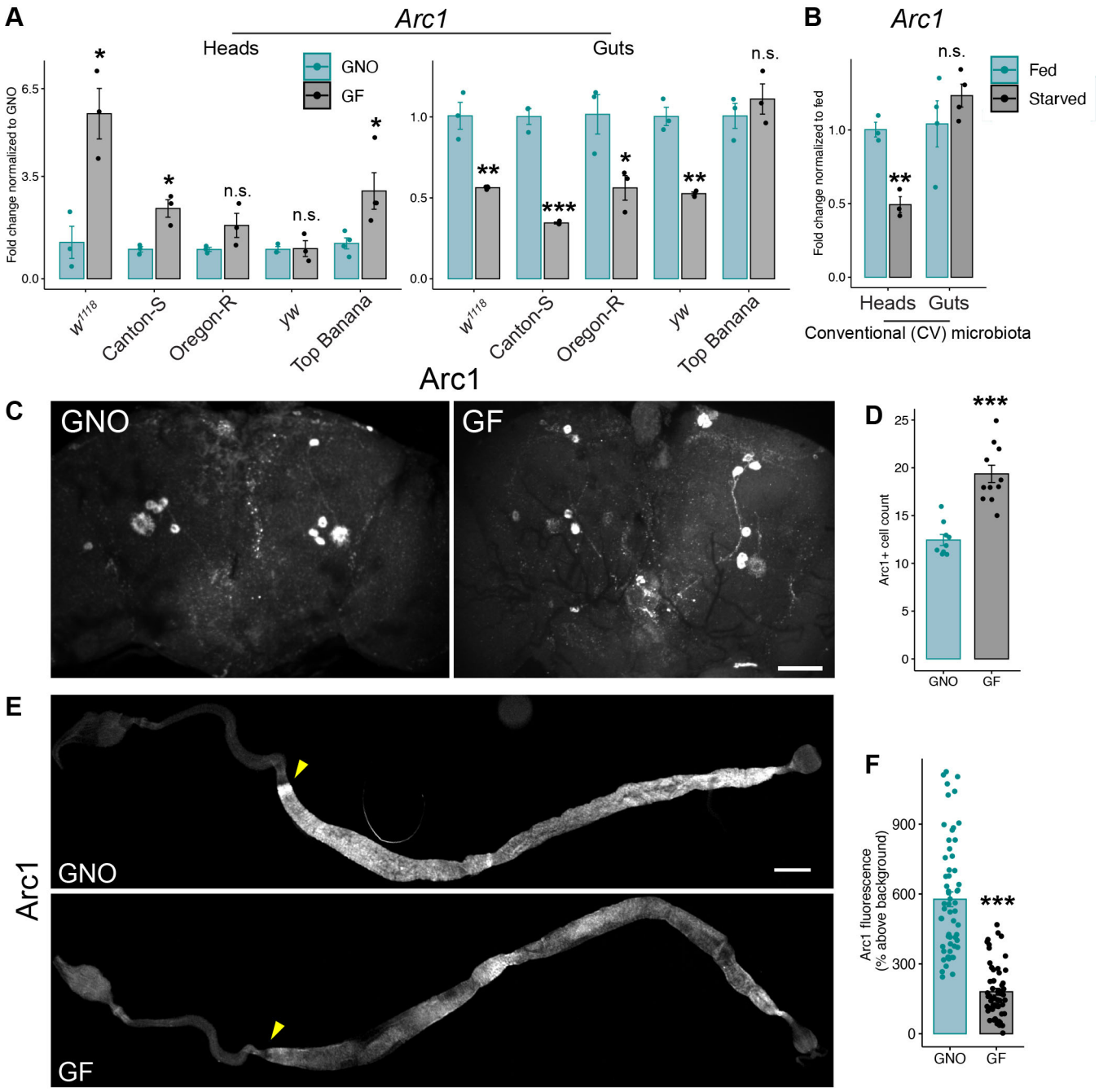

Fig. 1. Tissue-specific *Arc1* mRNA and protein responses to microbiota and nutrient deprivation. Five-day-old adult male w^{1118} flies were used for all analyses unless otherwise indicated. (A,B) RT-qPCR of *Arc1* transcripts in heads and guts of adults grown GNO or GF (A), and following 24 h starvation (B). In A, data are normalized to GNO condition for each genotype and in B data are normalized to fed condition for each tissue. Individual points represent normalized values for each replicate, ten animals per replicate, n=3-4. *P<0.05, **P<0.01, ***P<0.0001, n.s., not significant, unpaired, two-tailed Student's *t*-test. (C,D) Arc1 immunostaining (C) and quantification of the number of Arc1-positive cells (D) in adult posterior central brains under GF and GNO conditions. Scale bar: 10 µm. Points represent cell counts from individual animals, n=9-11. ***P<0.0001, unpaired, two-tailed Student's *t*-test. (E) Arc1 immunostaining in the gut of GF and GNO flies. Arrowheads indicate the midgut-hindgut boundary. Scale bar: 200 µm. (F) Arc1 fluorescence intensity above background in posterior midgut cells at the midgut-hindgut boundary. Each point represents an individual cell, with ten cells per animal, n=6 animals per condition. ***P<0.0001, Mann–Whitney test. Error bars represent s.e.m.

to a single bacterial taxon or to the collective effects of the community. To test this, we mono-associated wild-type and *Arc1* null larvae with each of the four bacteria and assessed time to pupariation. Association with either of the two *Lactobacillus* isolates or *A. pasteurianus* accelerated both wild-type and $Arc1^{E8}$ larval growth, but was not sufficient to promote growth to the same extent as the GNO community (Fig. 2F,G). In contrast, *Acetobacter* sp. was indistinguishable from GNO in promoting growth rate of both wild-type and $Arc1^{E8}$ animals (Fig. 2F,G). There were no significant differences in larval bacterial loads among the four

Development (2021) 148, dev195222. doi:10.1242/dev.195222

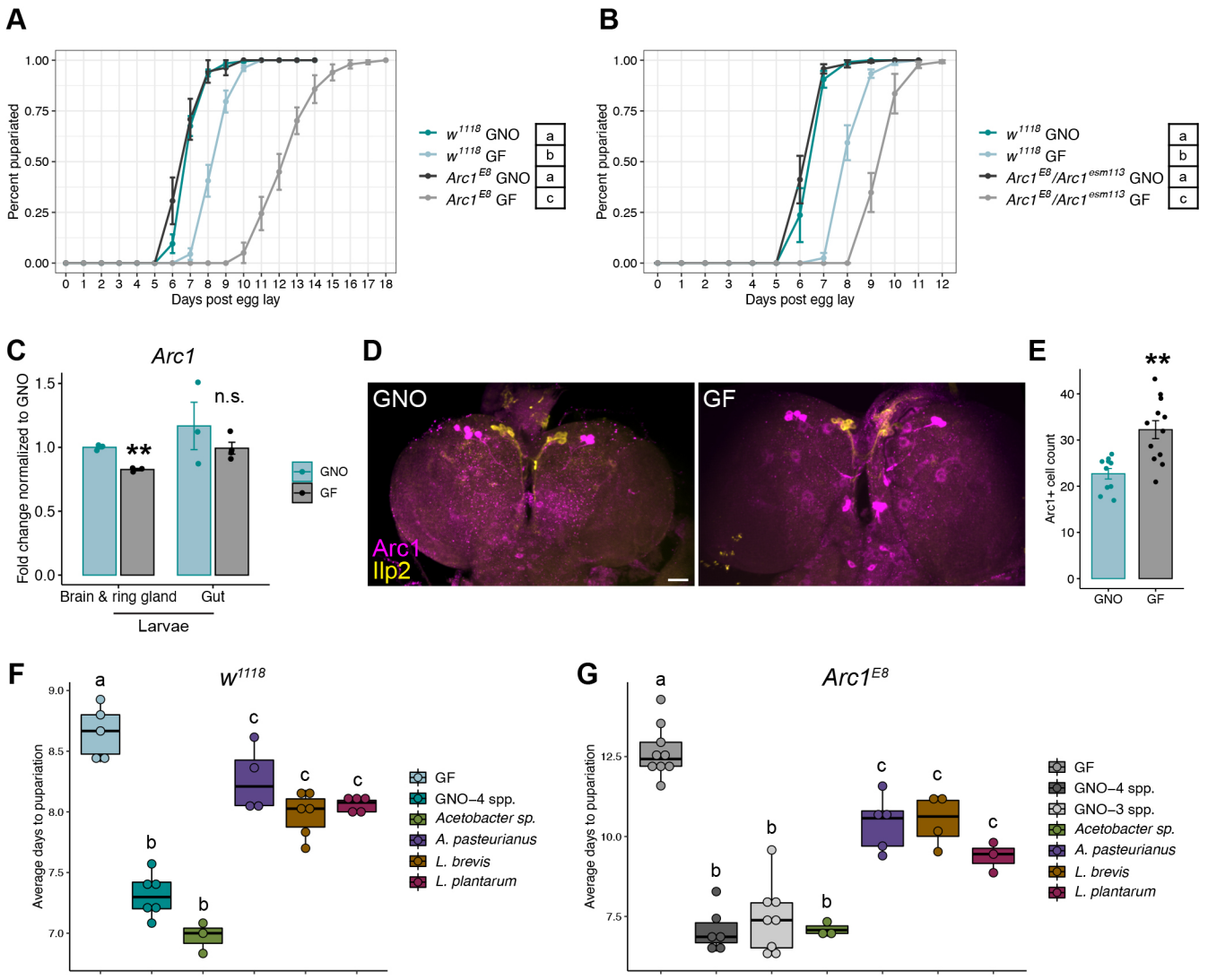

Fig. 2. Mono-association with *Acetobacter* sp. promotes growth rate of *Arc1* mutant larvae. (A,B) Time to pupariation for GNO and GF w^{1118} versus *Arc1* mutants. (C) RT-qPCR analysis of *Arc1* transcripts in the indicated larval tissues. Data normalized to GNO condition for each tissue. Individual points represent normalized values for each replicate, 10-20 animals per replicate, *n*=3-4. (D,E) Arc1 and Ilp2 immunostaining (D) and counts of Arc1-positive cells (E) in the central region of the larval brain. Scale bar: 5 µm. Points represent cell counts from individual animals, *n*=10-12. (F,G) Time to pupariation for wild-type and *Arc1* mutant animals mono-associated with each of the four bacterial isolates comprising the GNO-4spp. condition. GNO-3spp.: *A. pasteurianus*, *L. brevis* and *L. plantarum*. (C,E) ***P*<0.01, n.s., not significant, unpaired, two-tailed Student's *t*-test. Error bars represent s.e.m. Conditions sharing letters are not statistically different from one another, one-way (F,G) or two-way (A,B) ANOVA with Tukey's post-hoc test. For all developmental rate experiments, see Table S1 for full sample sizes and statistical results.

isolates that might explain the growth-promoting action of *Acetobacter* sp. (Fig. S4A).

Because *Acetobacter* sp. alone was sufficient to achieve a growth rate comparable to wild-type in $Arc1^{E8}$ larvae, we investigated whether it is also necessary in the four-species GNO community. Whereas mutant larvae associated with *A. pasteurianus*, *L. brevis* and *L. plantarum* individually developed substantially slower than those associated with the four-species group or *Acetobacter* sp., the three together in a GNO community lacking *Acetobacter* sp. were sufficient to promote normal development (GNO-3spp; Fig. 2G). For experimental tractability, we focused all subsequent investigation on larvae mono-associated with *Acetobacter* sp.

Although the delayed pupariation rate of wild-type GF larvae reflects a moderately extended duration of all three larval instars (Fig. S4B; Storelli et al., 2011), $Arc1^{E8}$ GF larvae underwent prolonged L1 and L2 phases (Fig. S4B). Further, GF animals of both genotypes increased in size at a more gradual rate than those with *Acetobacter* sp., but this effect was exaggerated in *Arc1* mutants, suggesting a longer time to attain the critical weight that triggers larval molts and metamorphosis (Fig. S4C; Mirth et al., 2005). The extended larval period could reflect reduced nutrient intake, but there were no differences in feeding behavior or food consumption (Fig. S4D,E).

Diet modulates the *Arc1*-dependent GF larval developmental delay

We demonstrated that *Arc1* loss significantly exacerbates the developmental delay of GF larvae. The developmental rate of wild-type GF larvae is particularly sensitive to dietary yeast, the primary source of ingested amino acids and many other nutrients (Piper et al., 2014; Shin et al., 2011; Storelli et al., 2011; Wong et al., 2014). To determine how *Arc1* deletion impacts microbe-dependent larval

Development (2021) 148, dev195222. doi:10.1242/dev.195222

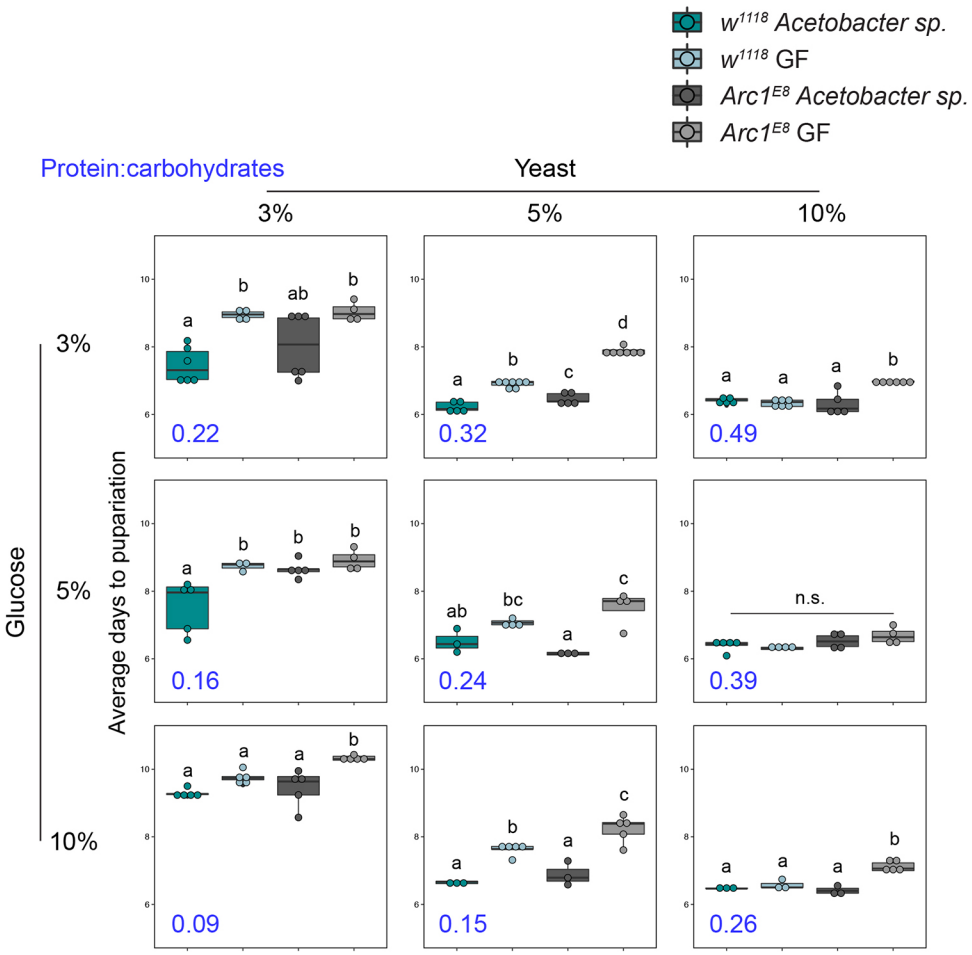

Fig. 3. Host diet impacts microbial effects on wild-type and *Arc1* mutant developmental rate. Time to pupariation for wild-type and *Arc1*^{E8} *Acetobacter* sp.-associated and GF larvae reared on diets consisting of the indicated concentrations (weight/volume) of yeast and dextrose. Values in blue represent the protein:carbohydrate ratio for each diet as calculated with the *Drosophila* Diet Composition Calculator (Lesperance and Broderick, 2020a). Conditions that share a letter are not statistically different from one another, n.s., not significant, two-way ANOVA with Tukey's post-hoc test.

dietary sensitivity, we monitored time to pupariation of *Acetobacter* sp.-associated and GF wild-type and *Arc1*^{E8} larvae fed nine yeast-dextrose diets of varying protein:carbohydrate ratios (Fig. 3; Lesperance and Broderick, 2020a).

As expected, in wild-type animals 'high-yeast' (10%) diets eliminated the developmental gap between *Acetobacter* sp.-associated and GF larvae, regardless of glucose concentration, whereas on 'low-yeast' (3%) diets wild-type GF larvae were consistently delayed. The exception to this was the 3% yeast-10% glucose diet, which substantially slowed the developmental rate of all conditions, a known effect of high-sugar, low-protein diets (Musselman et al., 2011; Wong et al., 2014). Interestingly, on 5% yeast diets, increasing glucose concentration moderately accelerated the development of wild-type GF larvae, with a delay observed only at the lowest glucose level.

GF larvae lacking *Arc1* generally showed enhanced developmental sensitivity to dietary composition; GF *Arc1*^{E8} animals developed more slowly than GF wild type on 5/9 diets tested, including 2/3 'high yeast' diets (Fig. 3). On most diets, *Acetobacter* sp.-associated *Arc1* mutants developed at the same rate as *Acetobacter* sp.-associated wild-type larvae. One exception was the 3% yeast-5% glucose diet, where *Acetobacter* sp. failed to have any growth rate-promoting activity for *Arc1*^{E8} larvae. Importantly, we did not find differences in *Acetobacter* sp. abundance on these diets that might correspond to the differences in growth rate of larvae of either genotype (Fig. S5).

Although GF *Arc1*-deficient larvae exhibited developmental delay on multiple diets, none of those tested yielded a magnitude of delay comparable to that on our laboratory's routine diet (protein:carbohydrate ratio 0.06; Fig. 2A). This may indicate that the full growth rate-promoting effects of *Acetobacter* sp. require the more complex cornmeal-yeast-molasses diet and are less dependent on the protein:carbohydrate ratio.

Together, these results indicate that the importance of *Arc1* function during GF larval development is dependent on the host's nutritional environment, and suggest that *Arc1* may be particularly important for GF larval growth dynamics in response to amino acid availability.

Live *Acetobacter* sp. populations are required for optimal *Arc1* mutant growth rate

We next investigated how *Acetobacter* sp. enables *Arc1*-deficient animals to develop at the same rate as wild-type mono-associated animals. We hypothesized that consumed bacteria may be a supplemental food source supporting *Arc1*^{E8} development, as reported in wild-type *Drosophila* (Bing et al., 2018; Keebaugh et al., 2018; Storelli et al., 2018). To test this, we inoculated GF wild-type and *Arc1*^{E8} cultures with heat-killed *Acetobacter* sp. cells daily throughout the larval growth period. This had no significant effect on GF wild-type or *Arc1* mutant larval developmental rates (Fig. 4A), providing no evidence for *Acetobacter* sp. cells as a nutritional supplement that affects growth.

The *Acetobacteraceae* generate acetic acid (Saichana et al., 2015), and two studies have shown that acetic acid/acetate consumption can accelerate the development of GF larvae or larvae associated with an acetic acid-deficient *Acetobacter* (Kamareddine et al., 2018; Shin et al., 2011). Acetic acid has also been reported to yield no effect on

Development (2021) 148, dev195222. doi:10.1242/dev.195222

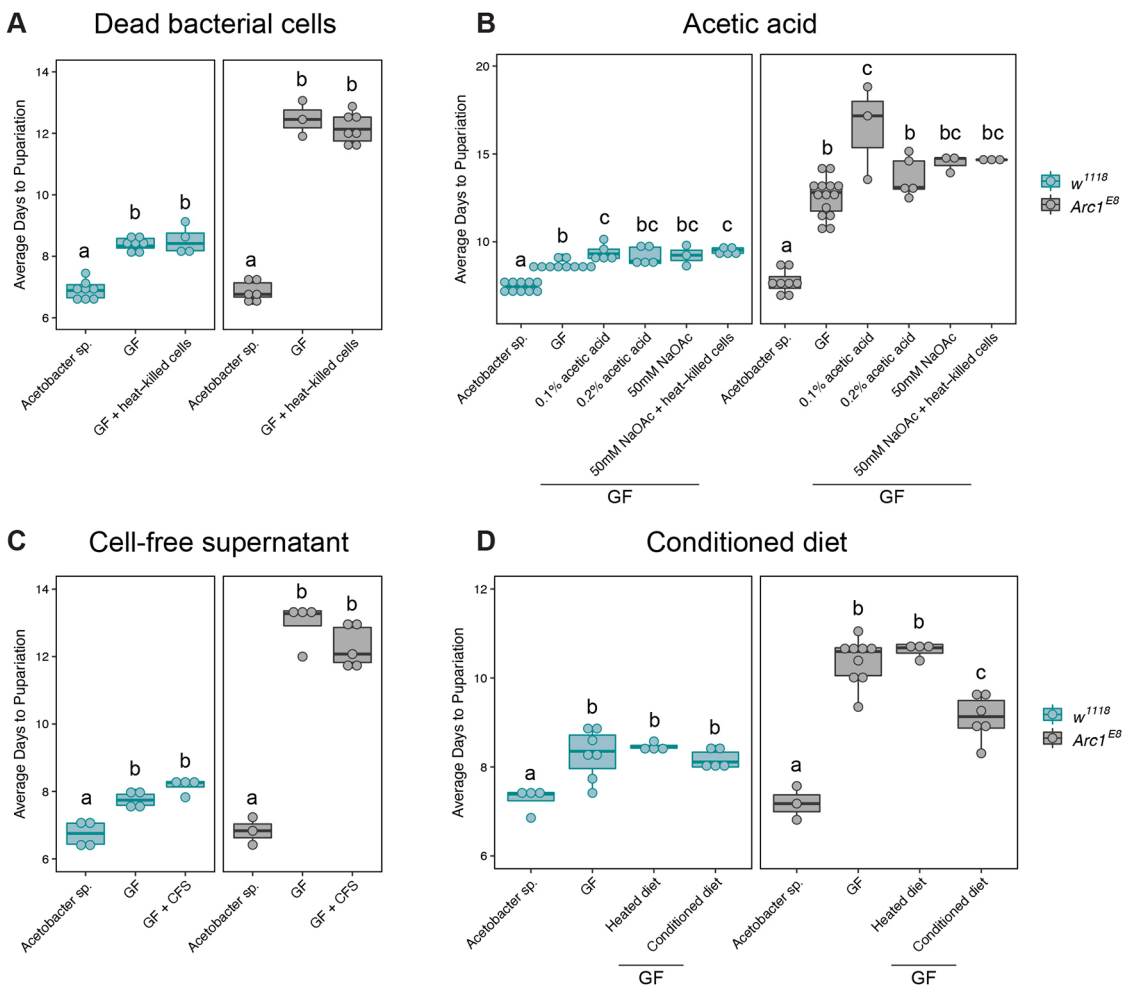

Fig. 4. *Acetobacter* sp.-conditioned diet accelerates the development of *Arc1* mutants. (A) Daily administration of heat-killed *Acetobacter* sp. planktonic culture has no effect on the developmental rate of GF wild-type or $Arc1^{E8}$ larvae. (B) Rearing GF wild-type and $Arc1^{E8}$ larvae on diets containing acetic acid either further extends or has no effect on the larval developmental delay. (C) Daily administration of filtered supernatant from *Acetobacter* sp. planktonic culture has no effect on developmental rate of GF wild-type or $Arc1^{E8}$ larvae. (D) Rearing GF larvae on a sterile diet that has been pre-conditioned with *Acetobacter* sp. for 5 days (Conditioned diet) has no effect on wild type, but partially restores the developmental rate of $Arc1^{E8}$ animals. Heated diet: GF diet heated under the same conditions used to kill *Acetobacter* sp. after pre-conditioning. Conditions that share a letter are not statistically different from one another, each panel analyzed by one-way ANOVA with Tukey's post-hoc test.

growth, or to exacerbate the GF developmental delay at higher concentrations (Kim et al., 2018; Shin et al., 2011). Consistent with the latter, we found that providing GF wild-type or $Arc1^{E8}$ larvae with dietary acetic acid either had no impact on growth rate, or further slowed larval development (Fig. 4B). Feeding GF larvae acetic acid-supplemented diet in combination with heat-killed cells also had no effect (Fig. 4B). Additionally, we found that daily inoculation with filtered supernatant from planktonic *Acetobacter* sp. cultures had no effect on either wild-type or $Arc1^{E8}$ GF larvae (Fig. 4C), suggesting that *Acetobacter* sp.-derived metabolite(s) do not promote growth.

Drosophila bacterial commensals proliferate on the flies' diet and are continually ingested (Ludington and Ja, 2020). The host and bacteria therefore share a dietary niche, with the bacteria utilizing the flies' food as a carbon source (Blum et al., 2013; Lesperance and Broderick, 2020b; Martino et al., 2018; Storelli et al., 2018). Certain microbe-dependent *Drosophila* traits, including growth rate, arise from bacterial utilization of dietary nutrients, producing an altered nutritional intake for the host (Consuegra et al., 2020; Huang and Douglas, 2015; Lesperance and Broderick, 2020b; Storelli et al., 2018). We therefore hypothesized that dietary modification might contribute to *Acetobacter* sp. support of *Arc1* mutant development. To test this, we inoculated GF food with *Acetobacter* sp., allowed colonization of the diet for 5 days, and then heat-killed all bacteria, resulting in an *Acetobacter* sp.-conditioned but microbiologically sterile food substrate.

The conditioned diet did not impact the developmental rate of wild-type GF larvae (Fig. 4D). In contrast, the conditioned diet substantially accelerated GF $Arc1^{E8}$ larval development, though these animals still developed at a significantly slower rate than *Arc1* mutants associated with live *Acetobacter* sp. (Fig. 4D). These data suggest that *Acetobacter* sp. modification of the larval diet is an important, though not exclusive, mechanism by which *Acetobacter* sp. promotes $Arc1^{E8}$ larval growth.

Acetobacter sp. ameliorates systemic metabolism-related *Arc1* mutant phenotypes

We next investigated whether the microbial environment impinges on other hallmarks of aberrant metabolism observed in *Arc1* mutants. Specifically, we assayed four organismal and cellular traits frequently associated with a larval growth delay and systemic metabolic dysregulation. In addition to slowed development, GF rearing stunts systemic growth yielding smaller pupae (Fig. 5A;

Development (2021) 148, dev195222. doi:10.1242/dev.195222

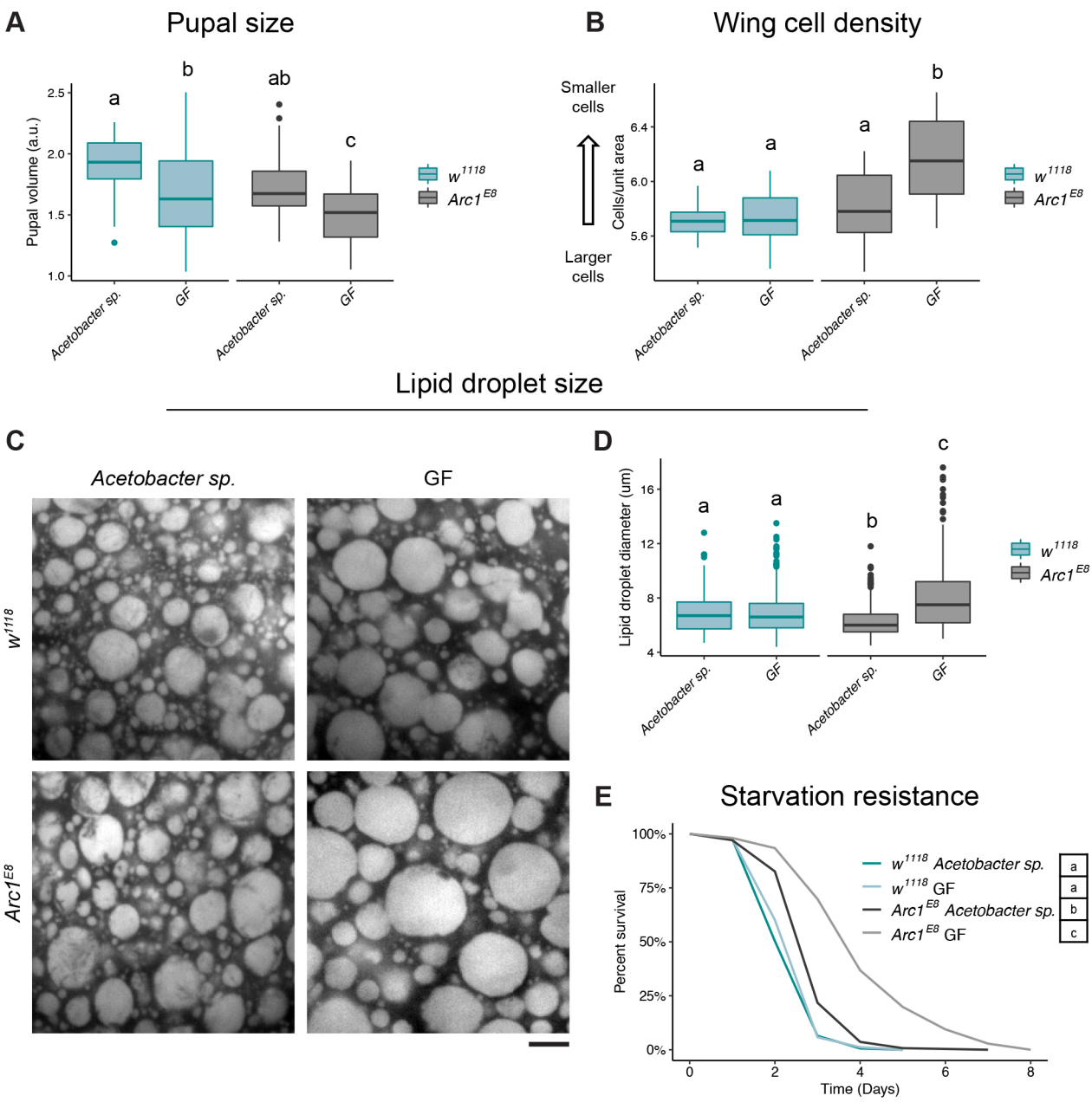

Fig. 5. GF *Arc1* mutants exhibit additional growth and metabolic defects that are suppressed by mono-association with *Acetobacter* sp. (A) Pupal volume is significantly decreased in GF *Arc1*^{E8} animals. *n*=34-63 pupae per condition. (B) Wing trichome density is increased (indicative of smaller cells) in GF *Arc1*^{E8} adult females. *n*=13-20 wings per condition. (C,D) Lipid droplet size is decreased in fat bodies of *Acetobacter* sp.-associated *Arc1*^{E8} larvae and increased in GF *Arc1*^{E8} larvae compared with wild-type animals under either microbial condition. *n*=407-512 lipid droplets from 15-20 animals per condition. Only droplets ≥5 µm were scored. Scale bar: 5 µm. (E) *Arc1*^{E8} mutants are more starvation resistant than wild type, and this is significantly enhanced in GF *Arc1*^{E8}. Conditions that share a letter are not statistically different from one another, Kruskal–Wallis test with Dunn's multiple comparison (A,B,D), Cox proportional-hazards model analysis (E).

Kamareddine et al., 2018; Storelli et al., 2018). This size reduction was exaggerated in GF *Arc1* mutants (Fig. 5A). Microbiota perturbation can also compromise cellular growth, as measured by cell size in the adult wing (Shin et al., 2011). Trichome density in adult wings was increased in GF *Arc1*^{E8} adults, indicating reduced cell size compared with wild-type animals of either microbial condition (Fig. 5B). These data are consistent with impaired systemic and cellular growth capacity upon loss of both *Arc1* and the microbiota.

Arc1 mutant larvae were previously shown to have elevated larval fat, and are starvation resistant as adults, the latter likely in part due to greater lipid stores accumulated during larval development (Mattaliano et al., 2007; Mosher et al., 2015). Consistent with these reports, we found that GF *Arc1* mutants had significantly larger lipid droplets in the larval fat body (the primary adipose tissue; Fig. 5C,D), and adult females survived full nutrient deprivation for ∼2 days longer than wild type (Fig. 5E).

Importantly, we primarily observed the effects of *Arc1* loss when *Arc1* mutants were reared GF; all four phenotypes were suppressed or altered when *Arc1* mutants were grown with *Acetobacter* sp. (Fig. 5). Interestingly, *Acetobacter* sp.-associated *Arc1*^{E8} larvae had significantly smaller lipid droplets in the fat

Development (2021) 148, dev195222. doi:10.1242/dev.195222

body compared with wild-type animals (Fig. 5D). Comparable to published results (Mattaliano et al., 2007), *Acetobacter* sp.-associated *Arc1* mutants were more starvation resistant than wild type, but succumbed considerably faster than GF mutants (Fig. 5E).

Collectively, these results indicate that loss of the microbiota uncovers or exacerbates growth and metabolic phenotypes in *Arc1*-deficient *Drosophila*, and association with a single bacterial taxon can strongly mitigate these defects.

Selective *Arc1* expression in neuroendocrine cells mitigates growth and metabolic defects

We next investigated the tissues in which Arc1 function is important for regulation of growth rate and other metabolism-related traits in GF animals. To this end, we selectively restored wild-type Arc1 in GF *Arc1*^{E8} flies using a *UAS-Arc1* transgene (Mattaliano et al., 2007) and a variety of GAL4 drivers expressed in organs/cell-types with known roles in growth regulation and/or where Arc1 is endogenously expressed.

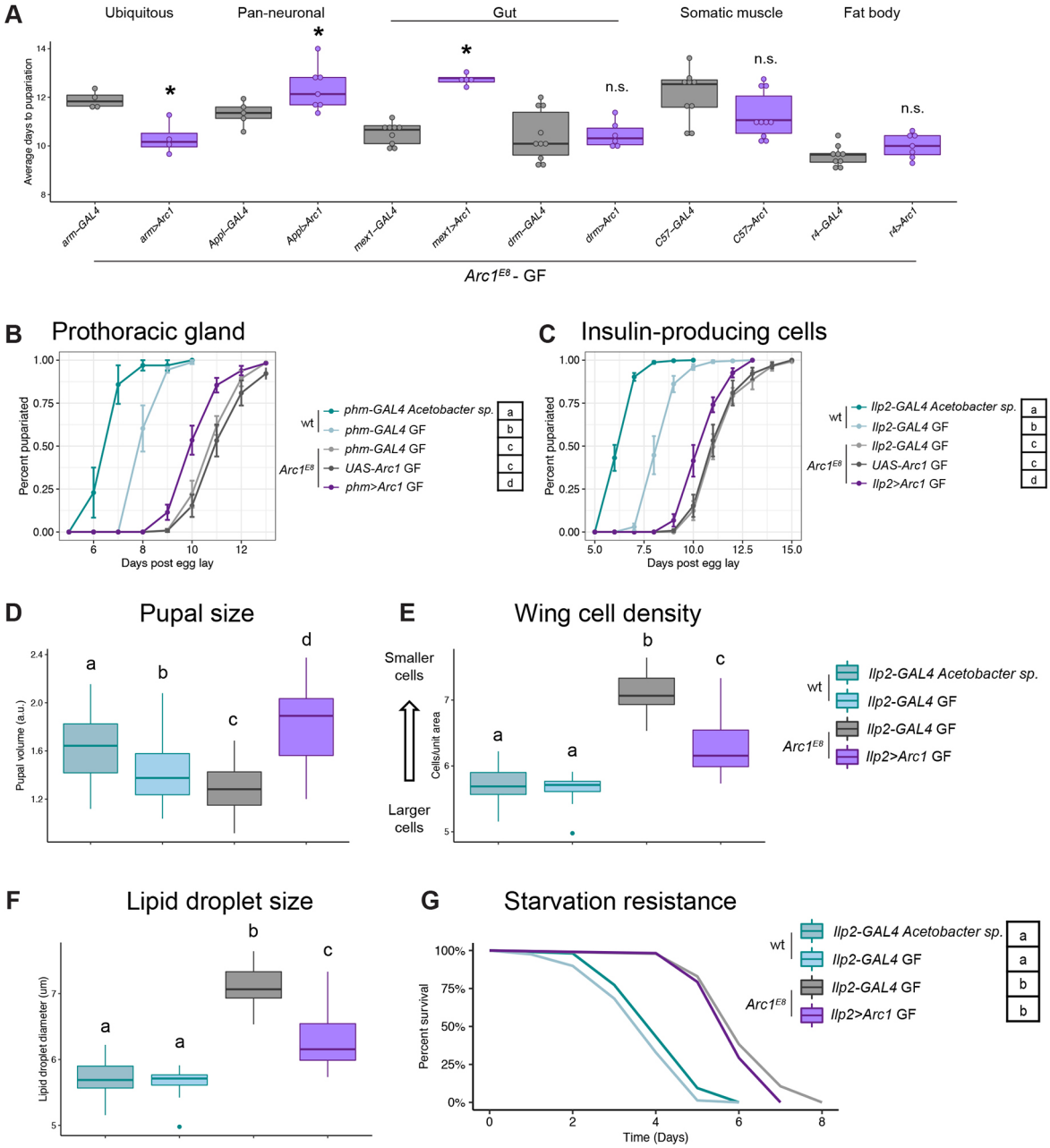

Fig. 6. Arc1 expression in multiple tissues impacts growth and metabolic traits. (A) Time to pupariation for GF *Arc1*^{E8} larvae with *Arc1* expression selectively restored in the indicated tissues. Individual points represent biological replicates. *P<0.05, n.s., not significant, one-way ANOVA with Tukey's post-hoc test. See Fig. S6 for full developmental rate growth curves and analyses. (B,C) Selectively expressing *Arc1* in the prothoracic gland (B) or the insulin-producing cells (IPCs, C) partially suppresses the *Arc1*^{E8}-GF developmental delay. (D) *Arc1* expression in the IPCs increases pupal size of *Arc1*^{E8}-GF animals even beyond that of the wild-type controls. n=42-55 pupae per condition. (E) *Arc1* IPC expression reduces increased trichome density (increases cell size) in *Arc1*^{E8}-GF adult female wings. n=10-44 wings per condition. (F) *Arc1* IPC expression reduces lipid droplet size in the *Arc1*^{E8}-GF larval fat body. n=489-673 lipid droplets from 12-16 animals per condition. (G) *Arc1* IPC expression does not affect starvation resistance under GF conditions. Conditions that share a letter are not statistically different from one another, one-way ANOVA with Tukey's post-hoc test (B,C,E), Kruskal–Wallis test with Dunn's multiple comparison (D,F), Cox proportional-hazards model analysis (G).

Development (2021) 148, dev195222. doi:10.1242/dev.195222

Weak ubiquitous (*armadillo-GAL4*) expression of *Arc1* significantly accelerated development in GF *Arc1*^{E8} larvae, whereas expression in the anterior midgut, hindgut and Malpighian tubules (*drumstick-GAL4*), somatic muscle (*C57-GAL4*) and fat body (*r4-GAL4*) had no effect (Fig. 6A, Fig. S6A-D). Interestingly, pan-neuronal *Arc1* expression (*Appl-GAL4*) or strong expression in the foregut and midgut (*mex1-GAL4*) further extended the growth delay in GF mutants (Fig. 6A, Fig. S6E,F).

Arc1 expression has been previously described in the ring gland (Mattaliano et al., 2007), a neuroendocrine organ that controls the timing of larval molts and pupariation through ecdysone biosynthesis (Mirth et al., 2005; Uryu et al., 2018; Yamanaka et al., 2015). Interestingly, Arc1 expression was strongly increased in the ring gland once larvae stopped feeding and starting wandering in preparation for pupariation (Fig. S7A-B″). Consistent with Arc1 playing a functional role in this growth-promoting tissue, selective expression of Arc1 in the prothoracic gland (PG) cells of the ring gland moderately but significantly suppressed the growth delay of GF *Arc1* mutants (Fig. 6B).

Larval growth is also systemically regulated by the production of insulin-like peptides (Ilps) in the insulin-producing cells (IPCs) of the larval brain (Géminard et al., 2009; Rulifson et al., 2002). In wild-type animals, clusters of strongly Arc1-positive neurons were observed lateral to the medial IPCs (Fig. 2D, Fig. S7C-D). Weakly Ilp2-positive cells sometimes could be observed adjacent to those Arc1-positive neurons (Fig. S7D, asterisks). Interestingly, in some cases, certain IPCs were weakly Arc1 positive (Fig. S7E-E″, arrowheads), and we found weaker Arc1-positive cells adjacent to the IPCs (Fig. S7F-F″, arrowheads). In the adult brain, Arc1 staining has been shown to fully colocalize with IPCs (Mattaliano et al., 2007). Overexpressing *Arc1* in the IPCs of GF *Arc1* null larvae (Fig. S7G-G″) significantly increased larval growth rate, but, as with selective expression in the PG, not to wild-type levels (Fig. 6C). Expressing *Arc1* in the IPCs also suppressed the reduced pupal size (Fig. 6D), reduced wing cell size (Fig. 6E) and enlarged lipid droplets (Fig. 6F), but did not alter the starvation resistance of GF *Arc1* mutants (Fig. 6G). Notably, ubiquitous, IPC-, and PG-specific overexpression of Arc1 had no effect on developmental rate or growth in GF wild-type larvae (Fig. S8A-D), whereas pan-neuronal and foregut-midgut overexpression exacerbated the GF developmental delay, similar to our observations in the *Arc1*^{E8} mutant background (Fig. S8E,F). Taken together, these data suggest that *Arc1* expression in multiple tissues is necessary to control larval growth and other metabolic traits.

Evidence for microbe-dependent and -independent changes in insulin and ecdysone pathways in Arc1-deficient larvae

We next sought to identify molecular changes in *Arc1* null animals that might yield mechanistic insight into their growth and metabolic defects. Collectively, the phenotypes we observed in GF *Arc1*^{E8} animals (Fig. 5) are reminiscent of those in IIS pathway mutants (Brogiolo et al., 2001; Broughton et al., 2005; DiAngelo and Birnbaum, 2009; Rulifson et al., 2002). For example, ablation of IPCs or loss of IIS signaling slows larval growth rate in GF or CV larvae (Fig. S9A; Rulifson et al., 2002). Surprisingly, we found that overactivation of IIS signaling in GF larvae through overexpression of Ilp2 or expression of activated PI3K also slows larval growth rate (Fig. S9B,C), similar to what has been previously described for overexpression of Ilp8 (Vallejo et al., 2015). Previous work did not reveal altered IIS function in *Arc1* mutants (Mattaliano et al., 2007; Mosher et al., 2015), though under different dietary conditions and without microbial manipulation (see Discussion). Notably, *Acetobacter* strains sustain larval growth by activating IIS in wild-type flies fed nutrient-restrictive diets (Kamareddine et al., 2018; Shin et al., 2011; Storelli et al., 2011). We therefore hypothesized that IIS function might be perturbed in a microbe-dependent manner in *Arc1*^{E8} larvae.

In adequately fed larvae, Ilps are synthesized in the IPCs and secreted into the hemolymph; decreased *Ilp* expression and Ilp retention in the brain are associated with nutritional deficiency and impaired growth promotion (Géminard et al., 2009). We found that *Ilp3* and *Ilp5*, but not *Ilp2*, transcripts were reduced ∼40% in the brains of feeding GF *Arc1*^{E8} larvae compared with wild-type *Acetobacter* sp.-associated larvae (Fig. 7A). Irrespective of these transcript level changes, both Ilp2 and Ilp5 protein levels were increased in *Acetobacter* sp.-associated *Arc1* mutant brains compared with GF *Arc1* mutant brains (Fig. 7B). Such accumulation is generally interpreted as evidence of decreased secretion and reduced IIS signaling.

Ilp secretion leads to systemic insulin signaling activation in key metabolic tissues, including the fat body (Brogiolo et al., 2001; DiAngelo and Birnbaum, 2009). Activation of IIS in these tissues leads to phosphorylation and activation of Akt (pAkt), nuclear exclusion of the transcription factor Foxo, and consequent upregulation of its negative targets *InR* and *Thor* (also known as *4E-BP*; Baker and Thummel, 2007). In GF *Arc1*^{E8} fat body lysates, pAkt was decreased compared with *Acetobacter* sp.-associated fat bodies, and trended lower than GF wild type, though the difference was not significant (Fig. 7C,D). Despite reduced pAkt levels (consistent with reduced IIS signaling), *InR* and *Thor* expression were either decreased (consistent with elevated IIS signaling) or unaffected in *Arc1*^{E8} fat bodies and whole animals, regardless of microbial condition (Fig. 7E,F). Interestingly, we observed the same trends of decreased pAkt and decreased Foxo target gene expression in wild-type GF animals (Fig. 7C-F).

Although we found that multiple IIS signaling steps are impacted by microbial condition and/or *Arc1* loss, these changes do not suggest simple increased or decreased IIS pathway activity in GF *Arc1*^{E8} larvae. This might indicate that the combined effects of *Arc1* and microbiota loss on IIS function are more complex than the effects of either manipulation alone, and thus could involve dysregulation of other pathways that impinge on IIS to affect metabolism and growth. The steroid hormone 20E regulates the timing of larval maturation, and is also nutrient responsive and intersects with IIS signaling (Boulan et al., 2013; Buhler et al., 2018; Yamanaka et al., 2015). Notably, the 20E biosynthetic pathway begins in the PG, where targeted *Arc1* expression suppresses the growth delay of GF *Arc1*^{E8} larvae (Fig. 6B). *shroud* (*sro*), a short-chain dehydrogenase/reductase that functions in this pathway in the PG (Niwa et al., 2010), was moderately decreased (∼35%) in larval brain/ring glands of feeding GF *Arc1*^{E8} animals, whereas transcripts of other ecdysone biosynthetic enzymes were unaffected (Fig. 7G). The monooxygenase *shade* (*shd*) converts ecdysone to bioactive 20E in the fat body (Petryk et al., 2003), and reduced *shade* expression delays pupariation, stunts growth, reduces *Ilp3* expression and induces Ilp2 retention (Buhler et al., 2018). Interestingly, fat body expression of *shade* decreased ∼50% in *Arc1* mutants under both microbial conditions (Fig. 7G).

Collectively, these data suggest that GF *Arc1* mutants experience complex dysregulation of two primary endocrine axes that regulate growth and metabolism in *Drosophila*, and some, but not all, of these defects are mitigated by *Acetobacter* sp.

Development (2021) 148, dev195222. doi:10.1242/dev.195222

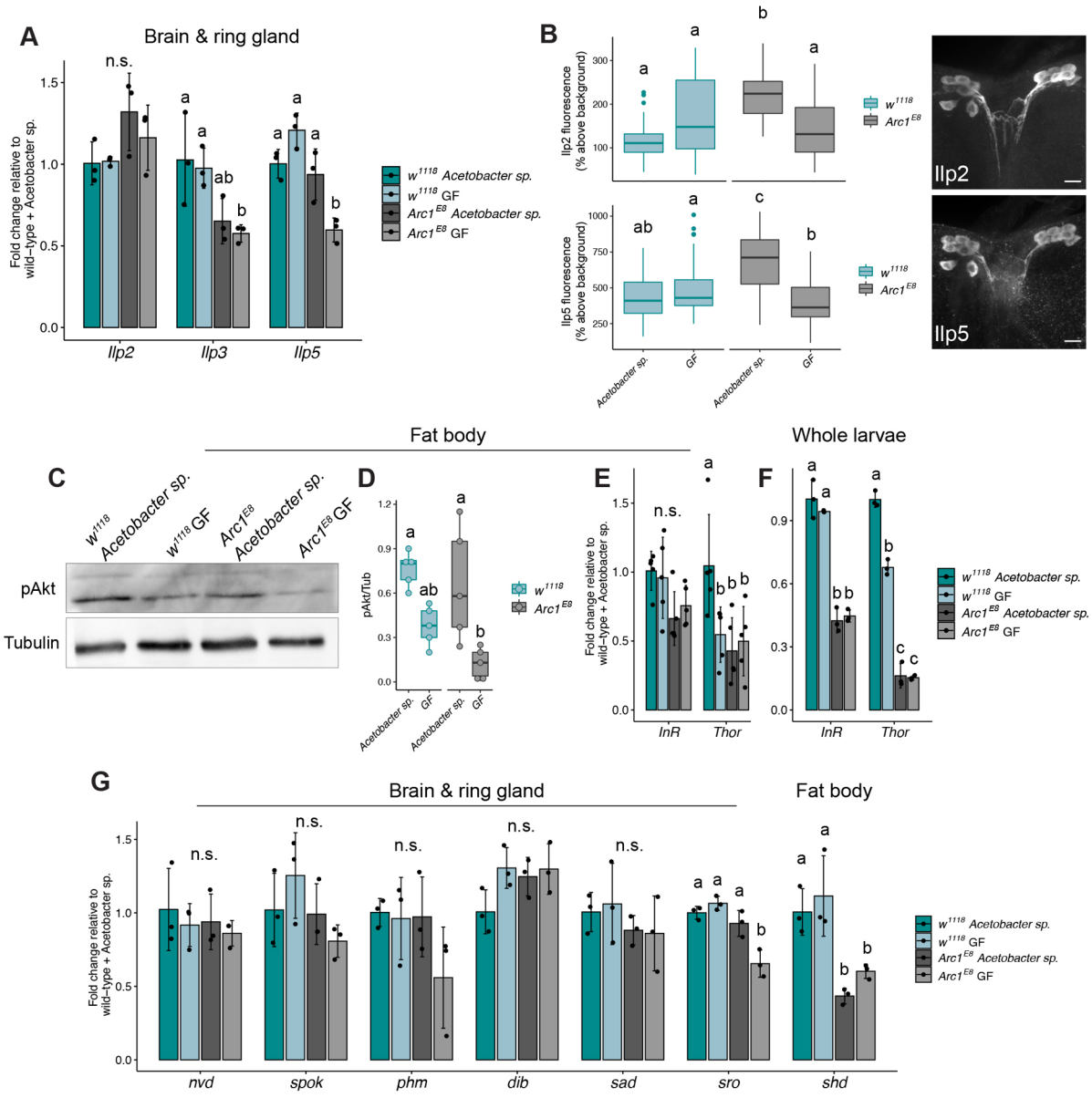

Fig. 7. Evidence of disrupted insulin and ecdysone signaling in GF *Arc1* mutants. (A) RT-qPCR analysis of insulin-like peptide (Ilp) gene expression in the brains of feeding *Acetobacter* sp.-associated and GF wild-type and $Arc1^{E8}$ larvae. (B) Ilp2 and Ilp5 protein levels are elevated in the insulin-producing cells (IPCs) of *Acetobacter* sp.-associated $Arc1^{E8}$ larvae and this is suppressed in GF animals. Representative images of Ilp2 and Ilp5 immunostaining in larval brain IPCs. Scale bars: 5 µm. (C,D) Phospho-Akt levels are reduced in the fat bodies of GF $Arc1^{E8}$ larvae compared with *Acetobacter* sp.-associated mutant and wild-type animals. (E,F) RT-qPCR of the insulin pathway target genes *InR* and *Thor* in the fat bodies of (E) or whole (F) feeding third instar larvae. (G) RT-qPCR of ecdysone biosynthetic genes in the brain/ring gland, and the monooxygenase enzyme shade (*shd*) in fat bodies of feeding larvae as indicated. Conditions that share a letter are not statistically different from one another, n.s., not significant, each panel analyzed by two-way ANOVA with Tukey's post-hoc test.

DISCUSSION

Many physiological traits in animals are shaped by highly complex, poorly understood interactions between a host's genotype and its microbiota. Here, we report an unexpected connection between the host gene *Arc1* and commensal bacteria that affects metabolism and growth in *Drosophila*. We initially identified *Arc1* from a screen for transcripts showing differential abundance in the heads of GF versus CV/GNO adult flies. Notably, *Arc1* was recently designated a 'core' microbiome-response gene in *Drosophila*, as it consistently appears in published RNA-seq studies focused on the gut or whole animals (Delbare et al., 2020). Our study further reveals that microbiota-dependent *Arc1* mRNA and protein changes vary in direction and magnitude between the gut and the head/brain, and among different populations of Arc1-positive cells in the brain (Figs 1 and 2, Figs S1 and S3). Arc1 expression increases substantially following neuronal activation, similar to mammalian Arc (Guan et al., 2005; Mattaliano et al., 2007; Montana and Littleton, 2006), and this response to activity can be brain region specific (Mosher et al., 2015), comparable to the microbiota-dependent cell type-specific variance we observed. Genetic manipulations that reduce IIS activity also yield tissue-specific differential *Arc1* expression (Musselman et al., 2018; Tain et al., 2021), as does rearing flies on a high-fat diet (Rivera et al., 2019) or under starved conditions (Fig. 1B).

Development (2021) 148, dev195222. doi:10.1242/dev.195222

Together, this complexity suggests that: (1) Arc1 expression is highly sensitive to microbial and nutritional cues, and (2) Arc1 might play mechanistically distinct roles in different tissues and cell types, necessitating precise spatiotemporal regulation of its transcript and protein levels. Consistent with the latter idea, targeted tissue-specific expression of Arc1 in *Arc1*^{E8} GF animals had a range of effects depending on the driver (Fig. 6, Fig. S6). Notably, overexpressing Arc1 pan-neuronally and in the foregut-midgut was deleterious, significantly exacerbating the GF growth delay of both wild-type and *Arc1* mutant larvae (Fig. 6A, Figs S6E,F and S8E,F). Although IPC-specific and PG-specific expression both accelerated GF *Arc1*^{E8} development, neither fully rescued the defect to wild-type GF growth rates (Fig. 6B,C). Similarly, IPC rescue only partially suppressed the reduced wing cell size and increased lipid droplet size of GF *Arc1* mutants, but resulted in pupae that were larger than wild-type animals, while having no impact on starvation resistance, in contrast to previous findings (Fig. 6D-G; Mattaliano et al., 2007). These results suggest that metabolic and growth homeostasis require precise modulation of Arc1 levels in multiple tissues. Also, Arc1 may function in mechanistically distinct ways in different tissues, with varying outcomes for the specific phenotypes we assayed. For example, *Arc1* transcript is abundant in wing imaginal discs (FlyAtlas; Leader et al., 2018), raising the possibility that Arc1 might have a cell-autonomous function in this tissue that contributes to wing cell size (Fig. 5B). To date, both *Drosophila* and mammalian Arc proteins have been studied primarily in the brain and neurons. Our work suggests that Arc proteins may play important roles in other organs and cell types, and this should be examined in vertebrate systems as well.

Despite its consistently reported microbe-dependent transcript changes, evidence for a functional interaction between Arc1 and the microbiota had not been previously investigated. We found that loss of *Arc1* in GF *Drosophila* resulted in deleterious phenotypes at the molecular, cellular and organismal levels that were all indicative of metabolic dysregulation and compromised growth (Figs 2, 5 and 7). Some of these findings are similar to previously reported *Arc1* mutant phenotypes, which suggested that Arc1 regulates systemic metabolism. Specifically, Mosher et al. (2015) showed that *Arc1*^{esm18} larvae have elevated whole-animal fat levels, which is consistent with our finding that GF *Arc1*^{E8} larvae have enlarged lipid droplets in the fat body (Fig. 5C,D). Mattaliano et al. (2007) reported that *Arc1*^{esm18} adults are starvation resistant, which we also observed in *Arc1*^{E8} adults (Fig. 5E). Importantly, as with developmental rate, pupal size and wing cell size (Figs 2A and 5A, B), we only observed these *Arc1* phenotypes (or, in the case of starvation resistance, observed the strongest effect) when *Arc1* mutants were also GF; *Arc1*^{E8} animals mono-associated with *Acetobacter* sp. were more similar to, if not indistinguishable from, wild-type animals in most of our assays. It should also be noted that our study and those mentioned above utilized considerably different diet formulations, and, in fact, we found that the microbe-dependent *Arc1* larval growth rate was extremely sensitive to diet (Fig. 3). These results highlight the need to consider diet and microbial condition as key factors that can interact strongly with host genotype to greatly influence phenotypic outcomes, in *Drosophila* and other model systems.

Although Arc1 was previously shown to impact systemic energy metabolism (Mosher et al., 2015), and our study has expanded the range of *Arc1* mutant phenotypes to include organismal and cellular growth defects, the exact molecular mechanisms through which Arc1 exerts these effects is unknown. Mammalian Arc promotes endocytosis of AMPA receptors via direct interactions with endocytic machinery (Chowdhury et al., 2006; DaSilva et al., 2016; Wall and Corrêa, 2018), and both *Drosophila* Arc1 and mammalian Arc encode polypeptides that can self-assemble into mRNA-containing capsid-like structures, which are released in extracellular vesicles and taken up by recipient cells (Ashley et al., 2018; Erlendsson et al., 2019; Pastuzyn et al., 2018). Both of these mechanisms appear to be crucial for the role of Arc as a master regulator of synaptic plasticity. Their potential contributions towards its metabolic and growth-promoting functions have not been investigated, but it is possible that distinct molecular functions dependent on cellular and tissue contexts may contribute to the role of Arc1 in metabolism and growth regulation.

The molecular and cellular processes impacted by the *Arc1*-microbiota-diet axis that might result in metabolic and growth phenotypes are also unclear. In *Drosophila*, these processes are largely coordinated by the intertwined activities of IIS and 20E signaling, which are both affected by the microbiota (Bing et al., 2018; Kamareddine et al., 2018; Shin et al., 2011; Storelli et al., 2011). Notably, we found that molecular readouts of IIS function at multiple points in the pathway, and in multiple tissues, were altered in *Arc1* mutants, though in both microbiota-dependent and -independent ways, and not consistent with simple IIS over- or under-activation (Fig. 7A-F). In addition to changes in the IIS pathway, two of the enzymes required for 20E biosynthesis are decreased in *Arc1* mutants (Fig. 7G). We think it is likely that the interplay between microbial condition and *Arc1* mutation has complex and multifarious impacts on many growth-regulating cellular processes, each of which may be a primary consequence of Arc1 loss, or secondary to the metabolic defects induced by Arc1 and microbiota removal. Interestingly, mammalian Arc has also been linked to insulin and metabolism. Arc expression can be strongly induced in cultured human neuroblasts by exogenous insulin (Kremerskothen et al., 2002), and mice fed a high-fat diet, which induces insulin resistance and diabetic-like phenotypes, have suppressed Arc expression in the cerebral cortex and hippocampus (Chen et al., 2020; Mateos et al., 2009). Our data suggest that links between Arc proteins and insulin signaling might be evolutionarily conserved, and that the influence of the microbiota may be an integral component of this relationship.

One of the major findings of this study is that mono-association with a single member of the bacterial microbiota, *Acetobacter* sp., was sufficient to fully or partially suppress most of the phenotypes observed in GF *Arc1* mutants. We further found that pre-conditioning the larval diet with *Acetobacter* sp. was sufficient to accelerate GF *Arc1*^{E8} development, suggesting that dietary modification is a key element of *Acetobacter* sp. growth-promoting activity (Fig. 4D). There is precedent for similar mechanisms in wild-type *Drosophila* associated with other microbiota members. For example, on nutritionally poor diets, *L. plantarum* depletes the levels of sugars and branched-chain amino acids, and increases the levels of glycolysis and fermentation products to promote larval growth (Storelli et al., 2018). Importantly, we found that live *Acetobacter* sp. populations are required for full growth rate promotion of *Arc1* mutants. In wild-type flies, commensal bacteria promote growth through interactions between bacterial cell wall components and gut cells, including induction of intestinal peptidase expression by D-alanylated teichoic acids (Consuegra et al., 2020; Matos et al., 2017), and innate immune signaling activation by DAP-type peptidoglycan (Davoodi et al., 2018; Kamareddine et al., 2018). Notably, these two modes of microbiota activity are reminiscent of microbial influence

Development (2021) 148, dev195222. doi:10.1242/dev.195222

on mammalian physiology. Bacterial breakdown of macronutrients, such as complex polysaccharides, in the human gut has been linked to health and disease states (Cockburn and Koropatkin, 2016). Other functions, such as immune cell maturation and maintenance of gut epithelial architecture, appear to require bacterial cell-derived antigens (Sekirov et al., 2010).

The ability of *Acetobacter* sp. to largely restore metabolic and developmental homeostasis to *Arc1* mutant *Drosophila* is a representative example of a bacterial symbiont mitigating the deleterious effects of genetic aberrations in the host, a prevalent feature of animal-microbe interactions (Douglas, 2019; Lynch and Hsiao, 2019; Ussar et al., 2016). The potential to harness these phenotypic buffering functions has motivated increasing efforts to develop microbial therapies for human diseases with a genetic basis (Baruch et al., 2021; Davar et al., 2021; Helmink et al., 2019). However, the success of these endeavors will require a more thorough understanding of the highly complex, modular interactions among host genotype, microbial metagenomes, diet, and other factors. This study reveals a tractable system in which to explore how a single host gene and the microbiota converge on conserved cellular pathways to regulate nutritional responsiveness, metabolic health and developmental growth.

MATERIALS AND METHODS

Drosophila stocks and diets

The following fly stocks were used: w^{1118}, Canton-S and Oregon-R are long-term lab stocks originally from the Bloomington *Drosophila* Stock Center (BDSC), Top Banana (derived from flies wild-caught in Seattle, Washington in 2013; kind gift from Dr Michael Dickinson; Giraldo et al., 2018), y^1w^1 (BDSC #1495), w^{1118}; $Arc1^{E8}$ (kind gift from Dr Vivian Budnik and Dr Travis Thomson, University of Massachusetts Medical School, USA), w^*;$Arc1^{esm113}$ (BDSC #37531), w^*;$Arc1^{esm18}$ (BDSC #37530), y^1w^{67c23};$Arc2^{EY21260}$ (BDSC #22466), w^*;;*UAS-Arc1-WT* (BDSC #37532), w^*;;*arm-Gal4* (BDSC #1561), *Appl-Gal4*,y^1w^* (BDSC #32040), w^{1118};;$Ilp2^{96A08}$-*GAL4* (BDSC #48030; Jenett et al., 2012), y^1w^*;;*phm-GAL4* (BDSC #80577), w^{1118};;*drm-GAL4* (BDSC #7098), *mex1-GAL4*,y^1w^* (kind gift from Dr Claire Thomas, Pennsylvania State University, USA), w^*;;*C57-GAL4* (BDSC #32556), y^1w^*;;*r4-GAL4* (BDSC #33832), w^*;;*Hs-GAL4* (BDSC #1799), y^1w^*;;*UAS-Ilp2* (BDSC #80936), w^{1118};*UAS-rpr* (BDSC #5824), *UAS-PI3K92E*^{CAAX},y^1w^{1118} (BDSC #8294). Additional mutations or transgenes present in *GAL4* stocks obtained from the BDSC were removed by standard crossing methods. We use a yeast-cornmeal-molasses diet consisting of (percentages given as wt/vol or vol/vol throughout): 8.5% molasses (Millhouse molasses; Domino Foods), 7% cornmeal (Enriched yellow cornmeal; Prairie Mills Products), 1.1% active dry yeast (Genesee Scientific 62-103), 0.86% gelidium agar (MoorAgar 41074), 0.27% propionic acid (Fisher Scientific A258) and 0.27% methylparaben (Sigma-Aldrich 47889). All experiments utilized this diet except those in Fig. 3, which were conducted on yeast-glucose diets. Yeast-glucose diets were prepared as described (Koyle et al., 2016) and consisted of the indicated proportions of active dry yeast and dextrose (Fisher Scientific BP350-1), with gelidium agar, propionic acid and methylparaben as above.

Bacterial stocks

The *Acetobacter* sp., *Acetobacter pasteurianus*, *Lactobacillus plantarum* and *Lactobacillus brevis* stocks utilized in this study were all isolated from conventionally reared Top Banana *Drosophila* cultures in our laboratory. Adult flies were surface sterilized in 10% bleach and 70% ethanol, rinsed three times and homogenized in PBS. Serial dilutions of fly homogenates were plated on de Man, Rogosa and Sharpe (MRS; Weber Scientific 3113-60) and acetic acid-ethanol (AE; Blum et al., 2013) agar plates: 0.8% yeast extract (Fisher Scientific 212750), 1.5% peptone (Fisher Scientific 211677), 1% dextrose, 0.5% ethanol, 0.3% acetic acid (Fisher Scientific A38-212). Colonies with distinct morphology were streaked for isolation. Bacterial taxonomies were assigned by PCR amplification and sequencing of the 16S rRNA gene using universal bacterial primers 8F (5′-AGAGTTTGATCTGGCTCAG-3′) and 1492R (5′-GGMTACCTTGTTACGACTT-3′; Eden et al., 1991). Sequences were searched against the NCBI nr/nt database via blastn (Altschul et al., 1990; Camacho et al., 2009; Morgulis et al., 2008) and taxonomies were assigned based on >97% sequence homology. Because the 16S rRNA sequence for isolate A22 (*Acetobacter* sp.) bore >97% similarity with more than five different *Acetobacter* species, we did not assign a species-level taxonomic classification.

Generation of GF and GNO fly cultures

GF and GNO *Drosophila* cultures were generated according to established methods (Koyle et al., 2016). Synchronous populations of embryos were collected on apple juice agar plates. In a sterile biosafety cabinet, embryos were treated with 50% bleach solution for 2 min to eliminate exogenous microbes and remove the chorion. Embryos were then rinsed twice in 70% ethanol, twice in sterilized milliQ water, and once in sterilized embryo wash: 2% Triton X-100 (MP Biomedicals 807426), 7% NaCl (Fisher Scientific BP358-212). Sterilized embryos were then pipetted into autoclaved food vials to generate GF cultures. To generate GNO flies, overnight cultures of bacterial isolates were grown for ∼16-18 h in MRS broth (30°C with shaking for *Acetobacter* isolates and 37°C static for *Lactobacilli*). Sterile food vials were inoculated with 40 µl of overnight cultures (OD∼1) immediately prior to the addition of sterilized fly embryos. For poly-associated (GNO) flies, vials were inoculated with 40 µl of a 1:1:1:1 mixture of overnight cultures of the four indicated bacteria.

For mono-association experiments (Fig. 2), bacterial inoculum was standardized to $\sim10^8$ colony-forming units (CFU) for each strain tested using the following empirically determined CFU/ml constants: *Acetobacter* sp.: 4.5×10^8; *A. pasteurianus*: 6.12×10^8; *L. brevis*: 4.28×10^8; *L. plantarum*: 1.14×10^8 (Koyle et al., 2016).

All experimental *Drosophila* cultures were maintained in an insect incubator at 23°C, 70% humidity, on a 12:12 light-dark cycle.

Larval and adult animals were confirmed as GF or mono-/poly-associated by homogenization in sterile PBS and plating on MRS and AE agar plates.

We did not maintain GF, GNO or mono-associated flies over multiple generations; all experiments utilized independently derived GF or GNO animals.

Developmental timing measurements

Synchronous populations of embryos were collected in a 4-6 h time window and treated as described above to generate cultures of defined microbial conditions. For pupariation and eclosion rate analysis, the number of pupae formed or empty pupal cases, respectively, were counted daily until 100% of the population had pupariated or eclosed. The duration of larval development is strongly affected by crowding conditions in the food (Klepsatel et al., 2018). Also, variable and unpredictable numbers of embryos do not survive the bleach and ethanol washes employed to generate GF and GNO cultures (Koyle et al., 2016; Troha and Buchon, 2019; S.A.K. and B.M.M., unpublished observations). We found that 10-30 larvae per vial was optimal for growth, and that within-treatment developmental rates were comparable for vials with larval densities in this range (see data provided in Peer Review History linked to this paper). Therefore, vials containing fewer than ten and greater than 30 animals were omitted from analyses as either under- or over-crowded, respectively.

Larval instars were determined via mouth hook and/or posterior spiracle morphologies (Bodenstein, 1950).

Larval length and pupal volume were measured from images using Fiji (Schindelin et al., 2012). For pupal volume, length (l) and width (w) of each pupa were measured and volume calculated as previously described (Layalle et al., 2008; Redhai et al., 2020): $V=4/3\pi(l/2)(w/2)^2$.

Larval feeding assays

Larval feeding was assessed via dye consumption (Buhler et al., 2018; Libert et al., 2007; Mosher et al., 2015; Shin et al., 2011). Pre-wandering third instar larvae were transferred to apple juice plates coated with dyed yeast paste consisting of a 2:1 mixture of 0.5% FD&C Red #40 dye (Ward's

Development (2021) 148, dev195222. doi:10.1242/dev.195222

Science 470301-004) and active dry yeast, and allowed to feed for 30 min at 23°C. Guts were then dissected from 20 larvae, homogenized in 1 ml PBS, and absorbance of the supernatant was measured at 490 nm with a Tecan Spark microplate reader.

Mouth hook contraction rates were assayed as described (Bhatt and Neckameyer, 2013). Pre-wandering third instar larvae were transferred to apple juice plates thinly coated with yeast paste, given 30 s to acclimate, and contractions were counted manually for 30 s.

Quantifying bacterial loads for mono-associated larvae

Pre-wandering third instar larvae (eight to ten animals per replicate) were removed from the food and surface sterilized in 10% bleach for 1 min. Larvae were then rinsed three times in PBS and homogenized in 125 µl PBS by bead beating for 30 s. Homogenates were serially diluted in PBS and dilutions were plated on AE (for *Acetobacter*) or MRS (for *Lactobacilli*) agar plates. Plates were incubated for 2-3 days at either 30°C (AE) or 37°C (MRS), and resultant colonies were counted manually from dilution plates bearing ∼50-400 colonies. Bacterial loads were calculated as CFU per larva, as previously described (Koyle et al., 2016), and log-transformed for analysis.

Dietary treatments

Heat-killed bacterial feeding (Fig. 4A)

Overnight cultures of *Acetobacter* sp. (culture density ∼2.5×10^8-10^9 CFU/ml) were heat-killed at 65°C for 3 h and autoclaved food vials were inoculated with 40 µl of heat-killed suspension prior to the addition of GF embryos. Vials were further inoculated with 40 µl heat-killed bacterial suspension daily until 100% of the population had pupariated. Successful heat-killing was confirmed for each daily inoculum by plating undiluted heat-treated bacterial suspension on AE plates, and by plating larval homogenates.

Acetic acid-supplemented diets (Fig. 4B)

Fly food was autoclaved and allowed to cool to ∼50-60°C. Glacial acetic acid (Fisher Scientific A38-212) was added to a final concentration of 0.1% or 0.2%, or sodium acetate (Sigma-Aldrich S2889) was added to a final concentration of 50 mM.

Cell-free supernatant feeding (Fig. 4C)

Overnight cultures of *Acetobacter* sp. (3 ml in MRS, grown as described above) were filtered twice through 0.22 µm PVDF sterile membrane filters (Genesee Scientific 25-240). Autoclaved food vials were inoculated with 40 µl of filtered media immediately prior to addition of GF embryos, and vials were further inoculated with 40 µl of filtered media daily until 100% of the population pupariated. Absence of live bacterial cells was confirmed by plating daily filtered media on AE plates, and plating larval homogenates.

Acetobacter sp.-conditioned diet (Fig. 4D)

Autoclaved food vials were inoculated with *Acetobacter* sp. overnight culture, as described above. Inoculated vials were incubated for 5 days at 23°C. Vials were then incubated at 65°C for 1 h to kill bacteria. Sterility of the conditioned diet was confirmed by plating food and larval homogenates on AE plates. Heated diet controls consisted of un-inoculated, autoclaved GF vials incubated at 65°C for 1 h.

Wing analysis

Wings from adult females were dissected, mounted in Aqua-mount (Thermo Scientific 14-390-5), and imaged with a QICAM-IR Fast 1394 camera (Q-Imaging) on a Zeiss Axioskop2 Plus microscope. Trichome density was measured with FijiWings2.3 software using the 150px trichome density feature (Dobens and Dobens, 2013).

Starvation resistance

Starvation experiments were conducted by transferring eight to ten 5-day-old adult females to 1% agar-water vials. Approximately 50-120 animals per condition per replicate were assessed. Flies were transferred to fresh agar-water vials daily and survival monitored daily until 100% of the population succumbed. Data from multiple replicates (two or three per condition) were combined for analysis.

RT-qPCR

Tissues were dissected in cold PBS and homogenized immediately in Trizol reagent (Thermo Fisher 15596026). RNA was extracted using the Direct-zol RNA Miniprep kit (Zymo Research 11-330) exactly following the manufacturer's protocol. High-quality RNA ($A_{260nm/280nm}$ ∼2; 250-500 ng) was used as template for cDNA synthesis using the qScript cDNA synthesis kit (QuantaBio 95048). Product from cDNA synthesis reactions was used for qPCR with PerfeCTa SYBR Green Supermix (QuantaBio 95055) in an Applied Biosystems 7300 Real Time PCR System instrument. Data were normalized to *Rpl32* and expression fold changes were calculated using the $2^{-\Delta\Delta Ct}$ method. Primer sequences are listed in Table S2.

Immunohistochemistry

For immunostaining of adult and larval brains and adult guts, tissues were dissected in cold PBS and fixed in 4% paraformaldehyde-PBS (Electron Microscopy Sciences 157-8) for 30 min at room temperature. Samples were washed in PBS with 0.3% Triton X-100 (PBT) and blocked for 1 h in PBS with 0.3% Triton X-100 and 5% normal goat serum (PNT; Invitrogen 10000C). Samples were then incubated with primary antibodies in PNT at 4°C overnight with agitation. After washing in PBT, samples were incubated with secondary antibodies in PNT for 3 h at room temperature. Samples were washed in PBS and mounted in aqua-poly/mount (Polysciences 18606) or ProLong Gold antifade mounting medium (Invitrogen P36934).

Primary antibodies were: rabbit anti-Arc1 (1:250; Ashley et al., 2018), rat anti-Ilp2 and rabbit anti-Ilp5 (1:800; Géminard et al., 2009), mouse anti-EcR common [1:100; Developmental Studies Hybridoma Bank (DSHB) DDA2.7]. Secondary antibodies were: Alexa Fluor 488-, Alexa Fluor 546- or Alexa Fluor 647-conjugated (1:1000; Invitrogen A32723, A11035, A48265).

For lipid droplet analysis, larval fat bodies were dissected in PBS, transferred to 6 mm-well Shandon multi-spot slides (Fisher Scientific 99-910-90) and fixed for 30 min in 4% paraformaldehyde-PBS. Fat bodies were then rinsed three times in PBS, incubated with BODIPY 493/503 (1 mg/ml; Invitrogen D3922) diluted 1:1000 in PBS for 30 min at room temperature, rinsed three times in PBS, and mounted as above.

Image acquisition and analysis

Images were captured on a spinning disk microscope with a Celesta 1 W light engine (Lumencor), an X-Light V2 scan head (Crest Optics), and a Prime95B CMOS camera (Photometrics) on a Zeiss Axiovert 200 M using Metamorph software (Molecular Devices).

All analyses were conducted using Fiji. Fluorescence intensity was calculated as the percentage fluorescence above background. Lipid droplets ≥5 µm were measured in a single *z*-plane that represented the largest diameter droplets between the tissue surface and the nuclei. Low-magnification images of adult guts (Fig. 1E) were stitched together manually using Fiji.

Western blots

Fat bodies from ten pre-wandering third instar larvae were dissected in PBS, homogenized by bead beating in 180 µl ice-cold PBS, and immediately frozen until analysis. Lysates were centrifuged at 16,000 ***g*** for 5 min to pellet tissue debris and equal volumes mixed 1:1 with 2× Laemmli sample buffer (Bio-Rad 161-0737). Samples were boiled, resolved on 10% SDS-PAGE gel, and transferred to 0.22 µm pore-size nitrocellulose membrane (Bio-Rad 1620112). Blots were blocked in 5% bovine serum albumin (Sigma-Aldrich BSAV-RO) in tris-buffered saline with 0.1% Tween 20 (TBS-T; Sigma-Aldrich 9416) and incubated overnight at 4°C with rabbit anti-phospho-Ser505-Akt (Cell Signaling Technology 4054) or mouse anti-α-Tubulin (DSHB 12G10) diluted 1:1000 in blocking buffer. Incubations with horseradish peroxidase-conjugated secondary antibodies (1:20,000; Jackson ImmunoResearch 111-035-003, 115-035-003) were performed for 3 h at room temperature, and signal detected with Pierce ECL substrate (Thermo Scientific 34580) on a ChemiDoc MP imaging system (Bio-Rad). Quantification of relative protein amounts was conducted using Fiji.

Statistical analyses

Statistical tests were conducted and figures generated using Prism 9 (GraphPad) and R version 3.5.1 (https://R-project.org). Except where noted, RT-qPCR and immunostaining data were analyzed using unpaired, two-tailed Student's *t*-test for comparison of two groups, or two-way ANOVA for comparison of genotype and microbial condition. For developmental rate data, the average time to pupariation was calculated for each vial from the number of individuals pupariating on each day until the entire population completed larval development. These per-vial values from at least three replicates were used for statistical analyses; full sample sizes and statistical test output for all development experiments are reported in Table S1. Within-genotype comparisons among different treatments were conducted using one-way analysis-of-variance (ANOVA), whereas comparisons among different genotypes and treatments were conducted via two-way ANOVA with Tukey's test used for post-hoc analysis. Data that did not meet parametric test assumptions (normal distribution assessed by Shapiro–Wilk test and homogeneity of variance assessed by Levene's test) were analyzed via Mann–Whitney test or Kruskal–Wallis test with Dunn's post-hoc comparison (Bonferroni correction). Tests used for each experiment are indicated in the figure legends. Starvation survival data were compared by Cox proportional-hazards model analysis using the 'survival' package (version 3.2-11, https://CRAN.R-project.org/package=survival). In all box-and-whisker plots, the box comprises two hinges around the median representing the first and third quartiles (the 25th and 75th percentiles). Upper whisker represents largest value no further than 1.5*inter-quartile range from the hinge. Lower whisker represents smallest value no further than 1.5*inter-quartile range. Outlying values beyond the whiskers are plotted as individual points. In figures, lowercase letters are used to indicate post-hoc statistical comparisons: conditions that share a letter are not statistically different from one another. Throughout, the threshold of statistical significance was considered $P<0.05$.

Acknowledgements

We thank members of the McCartney, Hiller and Mitchell labs for helpful discussions while conducting the study. We thank Rory Eutsey (Hiller lab, Carnegie Mellon University) for technical assistance with qPCR experiments. We would like to thank Dr John Woolford for providing feedback on the manuscript. The Top Banana fly stock was a generous gift from Dr Michael Dickinson's lab (CalTech). The Arc1E8 fly stock and Arc1 antibody were generous gifts from Dr Vivian Budnik and Dr Travis Thomson (University of Massachusetts Medical School). Mex1-GAL4 flies were a kind gift from Dr Claire Thomas (Pennsylvania State University). The Ilp2 and Ilp5 antibodies were generous gifts from Dr Pierre Léopold (Institut Curie). We thank the Bloomington *Drosophila* Stock Center for providing other fly stocks. We would like to thank the Woolford, Mitchell, Linstedt and Hinman labs, and the Molecular Biosensor and Imaging Center at Carnegie Mellon University for reagents and equipment.

Competing interests

The authors declare no competing or financial interests.

Author contributions

Conceptualization: S.A.K., B.M.M.; Validation: B.M.M.; Formal analysis: S.A.K., C.B., S.F., B.M.M.; Investigation: S.A.K., C.B., S.F., B.M.M.; Writing - original draft: S.A.K.; Writing - review & editing: B.M.M.; Visualization: S.A.K.; Supervision: B.M.M.; Project administration: B.M.M.; Funding acquisition: B.M.M.

Funding

Funding for this work was provided by a Charles E. Kaufman Foundation New Initiative Grant and a Carnegie Mellon University ProSEED/BrainHub seed grant (to B.M.M.). S.A.K. was supported by a National Science Foundation Graduate Research Fellowship (under grant numbers DGE 1252522 and DGE 1745016).

Peer review history

The peer review history is available online at https://journals.biologists.com/dev/article-lookup/doi/10.1242/dev.195222

References

Alhowikan, A. M. (2016). Activity-regulated cytoskeleton-associated protein dysfunction may contribute to memory disorder and earlier detection of autism spectrum disorders. *Med. Princ. Pract.* **25**, 350-354. doi:10.1159/000445351

Altschul, S. F., Gish, W., Miller, W., Myers, E. W. and Lipman, D. J. (1990). Basic local alignment search tool. *J. Mol. Biol.* **215**, 403-410. doi:10.1016/S0022-2836(05)80360-2

Ashley, J., Cordy, B., Lucia, D., Fradkin, L. G., Budnik, V. and Thomson, T. (2018). Retrovirus-like Gag protein Arc1 binds RNA and traffics across synaptic boutons. *Cell* **172**, 262-274.e11. doi:10.1016/j.cell.2017.12.022

Baker, K. D. and Thummel, C. S. (2007). Diabetic larvae and obese flies-emerging studies of metabolism in Drosophila. *Cell Metab.* **6**, 257-266. doi:10.1016/j.cmet.2007.09.002

Baruch, E. N., Wang, J. and Wargo, J. A. (2021). Gut microbiota and antitumor immunity: potential mechanisms for clinical effect. *Cancer Immunol. Res.* **9**, 365-370. doi:10.1158/2326-6066.CIR-20-0877

Bhatt, P. K. and Neckameyer, W. S. (2013). Functional analysis of the larval feeding circuit in Drosophila. *J. Vis. Exp.* **81**, e51062. doi:10.3791/51062

Bi, R., Kong, L.-L., Xu, M., Li, G.-D., Zhang, D.-F., Li, T., Fang, Y., Zhang, C., Zhang, B. and Yao, Y.-G. (2018). The arc gene confers genetic susceptibility to Alzheimer's disease in Han Chinese. *Mol. Neurobiol.* **55**, 1217-1226. doi:10.1007/s12035-017-0397-6

Bing, X. L., Gerlach, J., Loeb, G. and Buchon, N. (2018). Nutrient-dependent impact of microbes on Drosophila suzukii development. *MBio* **9**, e02199-17. doi:10.1128/mBio.02199-17

Blum, J. E., Fischer, C. N., Miles, J. and Handelsman, J. (2013). Frequent replenishment sustains the beneficial microbiome of Drosophila melanogaster. *MBio* **4**, e00860-13. doi:10.1128/mBio.00860-13

Bodenstein, D. (1950). The postembryonic development of Drosophila. In *Biology of Drosophila* (ed. M. Demerec), pp. 276-288. New York: John Wiley & Sons, Inc.

Bost, A., Franzenburg, S., Adair, K. L., Martinson, V. G., Loeb, G. and Douglas, A. E. (2017). How gut transcriptional function of *Drosophila melanogaster* varies with the presence and composition of the gut microbiota. *Mol. Ecol.* **27**, 1848-1859. doi:10.1111/mec.14413

Boulan, L., Martín, D. and Milán, M. (2013). Bantam miRNA promotes systemic growth by connecting insulin signaling and ecdysone production. *Curr. Biol.* **23**, 473-478. doi:10.1016/j.cub.2013.01.072

Broderick, N. A. and Lemaitre, B. (2012). Gut-associated microbes of *Drosophila melanogaster*. *Gut Microbes* **3**, 307-321. doi:10.4161/gmic.19896

Brogiolo, W., Stocker, H., Ikeya, T., Rintelen, F., Fernandez, R. and Hafen, E. (2001). An evolutionarily conserved function of the Drosophila insulin receptor and insulin-like peptides in growth control. *Curr. Biol.* **11**, 213-221. doi:10.1016/S0960-9822(01)00068-9

Broughton, S. J., Piper, M. D. W., Ikeya, T., Bass, T. M., Jacobson, J., Driege, Y., Martinez, P., Hafen, E., Withers, D. J., Leevers, S. J. et al. (2005). Longer lifespan, altered metabolism, and stress resistance in Drosophila from ablation of cells making insulin-like ligands. *Proc. Natl. Acad. Sci. USA* **102**, 3105-3110. doi:10.1073/pnas.0405775102

Buhler, K., Clements, J., Winant, M., Bolckmans, L., Vulsteke, V. and Callaerts, P. (2018). Growth control through regulation of insulin-signalling by nutrition-activated steroid hormone in drosophila. *Dev.* **145**, dev165654. doi:10.1242/dev.165654

Camacho, C., Coulouris, G., Avagyan, V., Ma, N., Papadopoulos, J., Bealer, K. and Madden, T. L. (2009). BLAST+: Architecture and applications. *BMC Bioinformatics* **10**, 421. doi:10.1186/1471-2105-10-421

Campillos, M., Doerks, T., Shah, P. K. and Bork, P. (2006). Computational characterization of multiple Gag-like human proteins. *Trends Genet.* **22**, 585-589. doi:10.1016/j.tig.2006.09.006

Carmichael, R. E. and Henley, J. M. (2018). Transcriptional and post-translational regulation of Arc in synaptic plasticity. *Semin. Cell Dev. Biol.* **77**, 3-9. doi:10.1016/j.semcdb.2017.09.007

Chaston, J. M., Newell, P. D. and Douglas, A. E. (2014). Metagenome-wide association of microbial determinants of host phenotype in Drosophila melanogaster. *MBio* **5**, e01631-14. doi:10.1128/mBio.01631-14

Chen, T. J., Chen, S. S., Wang, D. C. and Hung, H. S. (2020). High-fat diet reduces novelty-induced expression of activity-regulated cytoskeleton-associated protein. *J. Cell. Physiol.* **235**, 1065-1075. doi:10.1002/jcp.29021

Chowdhury, S., Shepherd, J. D., Okuno, H., Lyford, G., Petralia, R. S., Plath, N., Kuhl, D., Huganir, R. L. and Worley, P. F. (2006). Arc/Arg3.1 interacts with the endocytic machinery to regulate AMPA receptor trafficking. *Neuron.* **52**, 445-459. doi:10.1016/j.neuron.2006.08.033

Cockburn, D. W. and Koropatkin, N. M. (2016). Polysaccharide degradation by the intestinal microbiota and its influence on human health and disease. *J. Mol. Biol.* **428**, 3230-3252. doi:10.1016/j.jmb.2016.06.021

Consuegra, J., Grenier, T., Baa-Puyoulet, P., Rahioui, I., Akherraz, H., Gervais, H., Parisot, N., Da Silva, P., Charles, H., Calevro, F. et al. (2020). Drosophila-associated bacteria differentially shape the nutritional requirements of their host during juvenile growth. *PLoS Biol.* **18**, e3000681. doi:10.1371/journal.pbio.3000681

Cottee, M. A., Letham, S. C., Young, G. R., Stoye, J. P. and Taylor, I. A. (2019). Structure of Drosophila melanogaster ARC1 reveals a repurposed molecule with characteristics of retroviral Gag. *Sci. Adv.* **6**, eaay6354. doi:10.1126/sciadv.aay6354

DaSilva, L. L. P., Wall, M. J., de Almeida, L. P., Wauters, S. C., Januário, Y. C., Müller, J. and Corrêa, S. A. L. (2016). Activity-regulated cytoskeleton-associated protein controls AMPAR endocytosis through a direct interaction with clathrin-

adaptor protein 2. *eNeuro* **3**, ENEURO.0144-15.2016. doi:10.1523/ENEURO.0144-15.2016

Davar, D., Dzutsev, A. K., McCulloch, J. A., Rodrigues, R. R., Chauvin, J.-M., Morrison, R. M., Deblasio, R. N., Menna, C., Ding, Q., Pagliano, O. et al. (2021). Fecal microbiota transplant overcomes resistance to anti-PD-1 therapy in melanoma patients. *Science* **371**, 595-602. doi:10.1126/science.abf3363

Davoodi, S., Galenza, A., Panteluk, A., Deshpande, R., Ferguson, M., Grewal, S. and Foley, E. (2018). The immune deficiency pathway regulates metabolic homeostasis in Drosophila. *J. Immunol.* **202**, 2747-2759. doi:10.4049/jimmunol.1801632

Delbare, S. Y. N., Ahmed-Braimah, Y. H., Wolfner, M. F. and Clark, A. G. (2020). Interactions between the microbiome and mating influence the female's transcriptional profile in Drosophila melanogaster. *Sci. Rep.* **10**, 18168. doi:10.1038/s41598-020-75156-9

DiAngelo, J. R. and Birnbaum, M. J. (2009). Regulation of fat cell mass by insulin in Drosophila melanogaster. *Mol. Cell. Biol.* **29**, 6341-6352. doi:10.1128/MCB.00675-09

Dobens, A. C. and Dobens, L. L. (2013). Fijiwings: an open source toolkit for semiautomated morphometric analysis of insect wings. *G3* **3**, 1443-1449. doi:10.1534/g3.113.006676

Dobson, A. J., Chaston, J. M., Newell, P. D., Donahue, L., Hermann, S. L., Sannino, D. R., Westmiller, S., Wong, A. C.-N., Clark, A. G., Lazzaro, B. P. et al. (2015). Host genetic determinants of microbiota-dependent nutrition revealed by genome-wide analysis of Drosophila melanogaster. *Nat. Commun.* **6**, 6312. doi:10.1038/ncomms7312

Dobson, A. J., Chaston, J. M. and Douglas, A. E. (2016). The Drosophila transcriptional network is structured by microbiota. *BMC Genomics* **17**, 975. doi:10.1186/s12864-016-3307-9

Douglas, A. E. (2018). The Drosophila model for microbiome research. *Lab. Anim. (NY).* **47**, 157-164. doi:10.1038/s41684-018-0065-0

Douglas, A. E. (2019). Simple animal models for microbiome research. *Nat. Rev. Microbiol.* **17**, 764-775. doi:10.1038/s41579-019-0242-1

Eden, P. A. E., Schmidt, T. M., Blakemore, R. P. and Pace, N. R. (1991). Phylogenetic analysis of *Aquaspirillum magnetotacticum* using polymerase chain reaction-amplified 16S rRNA-specific DNA. *Int. J. Syst. Bacteriol.* **41**, 324-325. doi:10.1099/00207713-41-2-324

Edgar, B. A. (2006). How flies get their size: genetics meets physiology. *Nat. Rev. Genet.* **7**, 907-916. doi:10.1038/nrg1989

Erlendsson, S., Morado, D. R., Cullen, H. B., Shepherd, J. D. and Briggs, J. A. G. (2019). Structures of virus-like capsids formed by the drosophila neuronal Arc proteins. *Nat. Neurosci.* **23**, 172-175. doi:10.1038/s41593-019-0569-y

Fromer, M., Pocklington, A. J., Kavanagh, D. H., Williams, H. J., Dwyer, S., Gormley, P., Georgieva, L., Rees, E., Palta, P., Ruderfer, D. M. et al. (2014). De novo mutations in schizophrenia implicate synaptic networks. *Nature* **506**, 179-184. doi:10.1038/nature12929

Géminard, C., Rulifson, E. J. and Léopold, P. (2009). Remote control of insulin secretion by fat cells in Drosophila. *Cell Metab.* **10**, 199-207. doi:10.1016/j.cmet.2009.08.002

Gilbert, J. A., Krajmalnik-Brown, R., Porazinska, D. L., Weiss, S. J. and Knight, R. (2013). Toward effective probiotics for autism and other neurodevelopmental disorders. *Cell* **155**, 1446-1448. doi:10.1016/j.cell.2013.11.035

Giraldo, Y. M., Leitch, K. J., Ros, I. G., Warren, T. L., Weir, P. T. and Dickinson, M. H. (2018). Sun navigation requires compass neurons in Drosophila. *Curr. Biol.* **28**, 2845-2852.e4. doi:10.1016/j.cub.2018.07.002

Gnainsky, Y., Zfanya, N., Elgart, M., Omri, E., Brandis, A., Mehlman, T., Itkin, M., Malitsky, S., Adamski, J. and Soen, Y. (2021). Systemic regulation of host energy and oogenesis by microbiome-derived mitochondrial coenzymes. *Cell Rep.* **34**, 108583. doi:10.1016/j.celrep.2020.108583

Guan, Z., Saraswati, S., Adolfsen, B. and Littleton, J. T. (2005). Genome-wide transcriptional changes associated with enhanced activity in the Drosophila nervous system. *Neuron.* **48**, 91-107. doi:10.1016/j.neuron.2005.08.036

Guo, L., Karpac, J., Tran, S. L. and Jasper, H. (2014). PGRP-SC2 promotes gut immune homeostasis to limit commensal dysbiosis and extend lifespan. *Cell* **156**, 109-122. doi:10.1016/j.cell.2013.12.018

Guzowski, J. F., McNaughton, B. L., Barnes, C. A. and Worley, P. F. (1999). Environment-specific expression of the immediate-early gene Arc in hippocampal neuronal ensembles. *Nat. Neurosci.* **2**, 1120-1124. doi:10.1038/16046

Guzowski, J. F., Lyford, G. L., Stevenson, G. D., Houston, F. P., McGaugh, J. L., Worley, P. F. and Barnes, C. A. (2000). Inhibition of activity-dependent arc protein expression in the rat hippocampus impairs the maintenance of long-term potentiation and the consolidation of long-term memory. *J. Neurosci.* **20**, 3993-4001. doi:10.1523/JNEUROSCI.20-11-03993.2000

Hayes, C. L., Dong, J., Galipeau, H. J., Jury, J., McCarville, J., Huang, X., Wang, X.-Y., Naidoo, A., Anbazhagan, A. N., Libertucci, J. et al. (2018). Commensal microbiota induces colonic barrier structure and functions that contribute to homeostasis. *Sci. Rep.* **8**, 14184. doi:10.1038/s41598-018-32366-6

Helmink, B. A., Khan, M. A. W., Hermann, A., Gopalakrishnan, V. and Wargo, J. A. (2019). The microbiome, cancer, and cancer therapy. *Nat. Med.* **25**, 377-388. doi:10.1038/s41591-019-0377-7

Huang, J.-H. and Douglas, A. E. (2015). Consumption of dietary sugar by gut bacteria determines *Drosophila* lipid content. *Biol. Lett.* **11**, 20150469. doi:10.1098/rsbl.2015.0469

Jenett, A., Rubin, G. M., Ngo, T.-T. B., Shepherd, D., Murphy, C., Dionne, H., Pfeiffer, B. D., Cavallaro, A., Hall, D., Jeter, J. et al. (2012). A GAL4-driver line resource for Drosophila neurobiology. *Cell Rep.* **2**, 991-1001. doi:10.1016/j.celrep.2012.09.011

Judd, A. M., Matthews, M. K., Hughes, R., Veloz, M., Sexton, C. E. and Chaston, J. M. (2018). Bacterial methionine metabolism genes influence Drosophila melanogaster starvation resistance. *Appl. Environ. Microbiol.* **84**, e00662-18. doi:10.1128/AEM.00662-18

Kamareddine, L., Robins, W. P., Berkey, C. D., Mekalanos, J. J. and Watnick, P. I. (2018). The Drosophila immune deficiency pathway modulates enteroendocrine function and host metabolism. *Cell Metab.* **28**, 449-462.e5. doi:10.1016/j.cmet.2018.05.026

Keebaugh, E. S., Yamada, R., Obadia, B., Ludington, W. B. and Ja, W. W. (2018). Microbial quantity impacts Drosophila nutrition, development, and lifespan. *iScience* **4**, 247-259. doi:10.1016/j.isci.2018.06.004

Keith, S. A., Eutsey, R., Lee, H., Solomon, B., Oliver, S., Kingsford, C., Hiller, N. L. and McCartney, B. M. (2019). Identification of Microbiota-Induced Gene Expression Changes in the Drosophila melanogaster Head. *bioRxiv*.

Kim, G., Huang, J. H., McMullen, J. G., Newell, P. D. and Douglas, A. E. (2018). Physiological responses of insects to microbial fermentation products: insights from the interactions between Drosophila and acetic acid. *J. Insect Physiol.* **106**, 13-19. doi:10.1016/j.jinsphys.2017.05.005

Klepsatel, P., Procházka, E. and Gáliková, M. (2018). Crowding of Drosophila larvae affects lifespan and other life-history traits via reduced availability of dietary yeast. *Exp. Gerontol.* **110**, 298-308. doi:10.1016/j.exger.2018.06.016

Koyle, M. L., Veloz, M., Judd, A. M., Wong, A. C.-N., Newell, P. D., Douglas, A. E. and Chaston, J. M. (2016). Rearing the fruit fly Drosophila melanogaster under axenic and gnotobiotic conditions. *J. Vis. Exp.* **113**, 54219. doi:10.3791/54219

Kremerskothen, J., Wendholt, D., Teber, I. and Barnekow, A. (2002). Insulin-induced expression of the activity-regulated cytoskeleton-associated gene (ARC) in human neuroblastoma cells requires p21ras, mitogen-activated protein kinase/extracellular regulated kinase and src tyrosine kinases but is protein kinase C-independent. *Neurosci. Lett.* **321**, 153-156. doi:10.1016/S0304-3940(01)02532-0

Larsen, N., Vogensen, F. K., Van Den Berg, F. W. J., Nielsen, D. S., Andreasen, A. S., Pedersen, B. K., Al-Soud, W. A., Sørensen, S. J., Hansen, L. H. and Jakobsen, M. (2010). Gut microbiota in human adults with type 2 diabetes differs from non-diabetic adults. *PLoS ONE* **5**, e9085. doi:10.1371/journal.pone.0009085

Layalle, S., Arquier, N. and Léopold, P. (2008). The TOR pathway couples nutrition and developmental timing in Drosophila. *Dev. Cell* **15**, 568-577. doi:10.1016/j.devcel.2008.08.003

Leader, D. P., Krause, S. A., Pandit, A., Davies, S. A. and Dow, J. A. T. (2018). FlyAtlas 2: a new version of the Drosophila melanogaster expression atlas with RNA-Seq, miRNA-Seq and sex-specific data. *Nucleic Acids Res.* **46**, D809-D815. doi:10.1093/nar/gkx976

Lesperance, D. N. A. and Broderick, N. A. (2020a). Meta-analysis of Diets Used in Drosophila Microbiome Research and Introduction of the Drosophila Dietary Composition Calculator (DDCC). *G3* **10**, 2207-2211. doi:10.1534/g3.120.401235

Lesperance, D. N. A. and Broderick, N. A. (2020b). Gut bacteria mediate nutrient availability in Drosophila diets. *Appl. Environ. Microbiol.* **87**, e01401-e01420. doi:10.1128/AEM.01401-20

Libert, S., Zwiener, J., Chu, X., VanVoorhies, W., Roman, G. and Pletcher, S. D. (2007). Regulation of Drosophila life span by olfaction and food-derived odors. *Science* **315**, 1133-1137. doi:10.1126/science.1136610

Ludington, W. B. and Ja, W. W. (2020). Drosophila as a model for the gut microbiome. *PLoS Pathog.* **16**, e1008398. doi:10.1371/journal.ppat.1008398

Lynch, J. B. and Hsiao, E. Y. (2019). Microbiomes as sources of emergent host phenotypes. *Science* **365**, 1405-1409. doi:10.1126/science.aay0240

Ma, D., Bou-Sleiman, M., Joncour, P., Indelicato, C.-E., Frochaux, M., Braman, V., Litovchenko, M., Storelli, G., Deplancke, B. and Leulier, F. (2019). Commensal Gut bacteria buffer the impact of host genetic variants on Drosophila developmental traits under nutritional stress. *iScience* **19**, 436-447. doi:10.1016/j.isci.2019.07.048

Martino, M. E., Joncour, P., Leenay, R., Gervais, H., Shah, M., Hughes, S., Gillet, B., Beisel, C. and Leulier, F. (2018). Bacterial adaptation to the host's diet is a key evolutionary force shaping Drosophila-Lactobacillus symbiosis. *Cell Host Microbe* **24**, 109-119.e6. doi:10.1016/j.chom.2018.06.001

Mateos, L., Akterin, S., Gil-Bea, F.-J., Spulber, S., Rahman, A., Björkhem, I., Schultzberg, M., Flores-Morales, A. and Cedazo-Mínguez, A. (2009). Activity-regulated cytoskeleton-associated protein in rodent brain is down-regulated by high fat diet in vivo and by 27-hydroxycholesterol in vitro. *Brain Pathol.* **19**, 69-80. doi:10.1111/j.1750-3639.2008.00174.x

Matos, R. C., Schwarzer, M., Gervais, H., Courtin, P., Joncour, P., Gillet, B., Ma, D., Bulteau, A.-L., Martino, M. E., Hughes, S. et al. (2017). D-Alanylation of teichoic acids contributes to Lactobacillus plantarum-mediated Drosophila growth during chronic undernutrition. *Nat. Microbiol.* **2**, 1635-1647. doi:10.1038/s41564-017-0038-x

Mattaliano, M. D., Montana, E. S., Parisky, K. M., Littleton, J. T. and Griffith, L. C. (2007). The Drosophila ARC homolog regulates behavioral responses to starvation. *Mol. Cell. Neurosci.* **36**, 211-221. doi:10.1016/j.mcn.2007.06.008

McBrayer, Z., Ono, H., Shimell, M. J., Parvy, J.-P., Beckstead, R. B., Warren, J. T., Thummel, C. S., Dauphin-Villemant, C., Gilbert, L. I. and O'Connor, M. B. (2007). Prothoracicotropic hormone regulates developmental timing and body size in Drosophila. *Dev. Cell.* **13**, 857-871. doi:10.1016/j.devcel.2007.11.003

McFall-Ngai, M., Hadfield, M. G., Bosch, T. C. G., Carey, H. V., Domazet-Lošo, T., Douglas, A. E., Dubilier, N., Eberl, G., Fukami, T., Gilbert, S. F. et al. (2013). Animals in a bacterial world, a new imperative for the life sciences. *Proc. Natl. Acad. Sci. USA* **110**, 3229-3236. doi:10.1073/pnas.1218525110

Mirth, C., Truman, J. W. and Riddiford, L. M. (2005). The role of the prothoracic gland in determining critical weight for metamorphosis in Drosophila melanogaster. *Curr. Biol.* **15**, 1769-1807. doi:10.1016/j.cub.2005.09.017

Montana, E. S. and Littleton, J. T. (2006). Expression profiling of a hypercontraction-induced myopathy in Drosophila suggests a compensatory cytoskeletal remodeling response. *J. Biol. Chem.* **281**, 8100-8109. doi:10.1074/jbc.M512468200

Morgulis, A., Coulouris, G., Raytselis, Y., Madden, T. L., Agarwala, R. and Schäffer, A. A. (2008). Database indexing for production MegaBLAST searches. *Bioinformatics* **24**, 1757-1764. doi:10.1093/bioinformatics/btn322

Mosher, J., Zhang, W., Blumhagen, R. Z., D'Alessandro, A., Nemkov, T., Hansen, K. C., Hesselberth, J. R. and Reis, T. (2015). Coordination between Drosophila Arc1 and a specific population of brain neurons regulates organismal fat. *Dev. Biol.* **405**, 280-290. doi:10.1016/j.ydbio.2015.07.021

Musselman, L. P., Fink, J. L., Narzinski, K., Ramachandran, P. V., Hathiramani, S. S., Cagan, R. L. and Baranski, T. J. (2011). A high-sugar diet produces obesity and insulin resistance in wild-type Drosophila. *Dis. Model. Mech.* **4**, 842-849. doi:10.1242/dmm.007948

Musselman, L. P., Fink, J. L., Maier, E. J., Gatto, J. A., Brent, M. R. and Baranski, T. J. (2018). Seven-up is a novel regulator of insulin signaling. *Genetics.* **208**, 1643-1656. doi:10.1534/genetics.118.300770

Niwa, R., Namiki, T., Ito, K., Shimada-Niwa, Y., Kiuchi, M., Kawaoka, S., Kayukawa, T., Banno, Y., Fujimoto, Y., Shigenobu, S. et al. (2010). Non-molting glossy/shroud encodes a short-chain dehydrogenase/reductase that functions in the "Black Box" of the ecdysteroid biosynthesis pathway. *Development* **137**, 1991-1999. doi:10.1242/dev.045641

Pastuzyn, E. D., Day, C. E., Kearns, R. B., Kyrke-Smith, M., Taibi, A. V., McCormick, J., Yoder, N., Belnap, D. M., Erlendsson, S., Morado, D. R. et al. (2018). The neuronal gene arc encodes a repurposed retrotransposon Gag protein that mediates intercellular RNA transfer. *Cell* **172**, 275-288.e18. doi:10.1016/j.cell.2017.12.024

Petkau, K., Ferguson, M., Guntermann, S. and Foley, E. (2017). Constitutive immune activity promotes tumorigenesis in drosophila intestinal progenitor cells. *Cell Rep.* **20**, 1784-1793. doi:10.1016/j.celrep.2017.07.078

Petryk, A., Warren, J. T., Marqués, G., Jarcho, M. P., Gilbert, L. I., Kahler, J., Parvy, J.-P., Li, Y., Dauphin-Villemant, C. and O'Connor, M. B. (2003). Shade is the Drosophila P450 enzyme that mediates the hydroxylation of ecdysone to the steroid insect molting hormone 20-hydroxyecdysone. *Proc. Natl. Acad. Sci. USA* **100**, 13773-13778. doi:10.1073/pnas.2336088100

Piper, M. D. W., Blanc, E., Leitão-Gonçalves, R., Yang, M., He, X., Linford, N. J., Hoddinott, M. P., Hopfen, C., Soultoukis, G. A., Niemeyer, C. et al. (2014). A holidic medium for Drosophila melanogaster. *Nat. Methods* **11**, 100-105. doi:10.1038/nmeth.2731

Redhai, S., Pilgrim, C., Gaspar, P., van Giesen, L., Lopes, T., Riabinina, O., Grenier, T., Milona, A., Chanana, B., Swadling, J. B. et al. (2020). An intestinal zinc sensor regulates food intake and developmental growth. *Nature* **580**, 263-268. doi:10.1038/s41586-020-2111-5

Rivera, O., McHan, L., Konadu, B., Patel, S., Sint Jago, S. and Talbert, M. E. (2019). A high-fat diet impacts memory and gene expression of the head in mated female Drosophila melanogaster. *J. Comp. Physiol. B* **189**, 179-198. doi:10.1007/s00360-019-01209-9

Robertson, R. C., Manges, A. R., Finlay, B. B. and Prendergast, A. J. (2019). The human microbiome and child growth – first 1000 days and beyond. *Trends Microbiol.* **27**, 131-147. doi:10.1016/j.tim.2018.09.008

Rulifson, E. J., Kim, S. K. and Nusse, R. (2002). Ablation of insulin-producing neurons in flies: growth and diabetic phenotypes. *Science* **296**, 1118-1120. doi:10.1126/science.1070058

Saichana, N., Matsushita, K., Adachi, O., Frébort, I. and Frebortova, J. (2015). Acetic acid bacteria: a group of bacteria with versatile biotechnological applications. *Biotechnol. Adv.* **33**, 1260-1271. doi:10.1016/j.biotechadv.2014.12.001

Sampson, T. R. and Mazmanian, S. K. (2015). Control of brain development, function, and behavior by the microbiome. *Cell Host Microbe* **17**, 565-576. doi:10.1016/j.chom.2015.04.011

Sannino, D. R., Dobson, A. J., Edwards, K., Angert, E. R. and Buchon, N. (2018). The Drosophila melanogaster Gut microbiota provisions thiamine to its host. *MBio* **9**, e00155-18. doi:10.1128/mBio.00155-18

Schindelin, J., Arganda-Carreras, I., Frise, E., Kaynig, V., Longair, M., Pietzsch, T., Preibisch, S., Rueden, C., Saalfeld, S., Schmid, B. et al. (2012). Fiji: an open-source platform for biological-image analysis. *Nat. Methods.* **9**, 676-682. doi:10.1038/nmeth.2019

Sekirov, I., Russell, S. L., Antunes, L. C. M. and Finlay, B. B. (2010). Gut microbiota in health and disease. *Physiol. Rev.* **90**, 859-904. doi:10.1152/physrev.00045.2009

Shandilya, M. C. V. and Gautam, A. (2020). Hippocampal Arc induces decay of object recognition memory in male mice. *Neuroscience.* **431**, 193-204. doi:10.1016/j.neuroscience.2020.02.012

Shen, J., Obin, M. S. and Zhao, L. (2013). The gut microbiota, obesity and insulin resistance. *Mol. Aspects Med.* **34**, 39-58. doi:10.1016/j.mam.2012.11.001

Shepherd, J. D. and Bear, M. F. (2011). New views of Arc, a master regulator of synaptic plasticity. *Nat. Neurosci.* **14**, 279-284. doi:10.1038/nn.2708

Shin, S. C., Kim, S.-H., You, H., Kim, B., Kim, A. C., Lee, K.-A., Yoon, J.-H., Ryu, J.-H. and Lee, W.-J. (2011). Drosophila microbiome modulates host developmental and metabolic homeostasis via insulin signaling. *Science.* **334**, 670-674. doi:10.1126/science.1212782

Smith, K., McCoy, K. D. and Macpherson, A. J. (2007). Use of axenic animals in studying the adaptation of mammals to their commensal intestinal microbiota. *Semin. Immunol.* **19**, 59-69. doi:10.1016/j.smim.2006.10.002

Storelli, G., Defaye, A., Erkosar, B., Hols, P., Royet, J. and Leulier, F. (2011). Lactobacillus plantarum promotes drosophila systemic growth by modulating hormonal signals through TOR-dependent nutrient sensing. *Cell Metab.* **14**, 403-414. doi:10.1016/j.cmet.2011.07.012

Storelli, G., Strigini, M., Grenier, T., Bozonnet, L., Schwarzer, M., Daniel, C., Matos, R. and Leulier, F. (2018). Drosophila perpetuates nutritional mutualism by promoting the fitness of its intestinal symbiont Lactobacillus plantarum. *Cell Metab.* **27**, 362-377. doi:10.1016/j.cmet.2017.11.011

Strigini, M. and Leulier, F. (2016). The role of the microbial environment in *Drosophila* post-embryonic development. *Dev. Comp. Immunol.* **64**, 39-52. doi:10.1016/j.dci.2016.01.017

Tain, L. S., Sehlke, R., Meilenbrock, R. L., Leech, T., Paulitz, J., Chokkalingam, M., Nagaraj, N., Grönke, S., Fröhlich, J., Atanassov, I., et al. (2021). Tissue-specific modulation of gene expression in response to lowered insulin signalling in *Drosophila*. *eLife* **10**, e67275. doi:10.7554/eLife.67275

Troha, K. and Buchon, N. (2019). Methods for the study of innate immunity in Drosophila melanogaster. *Wiley Interdiscip. Rev. Dev. Biol.* **9**, e344. doi:10.1002/wdev.344

Uryu, O., Ou, Q., Komura-Kawa, T., Kamiyama, T., Iga, M., Syrzycka, M., Hirota, K., Kataoka, H., Honda, B. M., King-Jones, K. et al. (2018). Cooperative control of ecdysone biosynthesis in drosophila by transcription factors séance, ouija board, and molting defective. *Genetics* **208**, 605-622. doi:10.1534/genetics.117.300268

Ussar, S., Fujisaka, S. and Kahn, C. R. (2016). Interactions between host genetics and gut microbiome in diabetes and metabolic syndrome. *Mol. Metab.* **5**, 795-803. doi:10.1016/j.molmet.2016.07.004

Vallejo, D. M., Juarez-Carreño, S., Bolivar, J., Morante, J. and Dominguez, M. (2015). A brain circuit that synchronizes growth and maturation revealed through Dilp8 binding to Lgr3. *Science* **350**, aac6767. doi:10.1126/science.aac6767

Wall, M. J. and Corrêa, S. A. L. (2018). The mechanistic link between Arc/Arg3.1 expression and AMPA receptor endocytosis. *Semin. Cell Dev. Biol.* **77**, 17-24. doi:10.1016/j.semcdb.2017.09.005

Wat, L. W., Chao, C., Bartlett, R., Buchanan, J. L., Millington, J. W., Chih, H. J., Chowdhury, Z. S., Biswas, P., Huang, V., Shin, L. J. et al. (2020). A role for triglyceride lipase brummer in the regulation of sex differences in Drosophila fat storage and breakdown. *PLoS Biol.* **18**, e3000595. doi:10.1371/journal.pbio.3000595

Wong, A. C.-N., Dobson, A. J. and Douglas, A. E. (2014). Gut microbiota dictates the metabolic response of Drosophila to diet. *J. Exp. Biol.* **217**, 1894-1901. doi:10.1242/jeb.101725

Yamanaka, N., Marqués, G. and O'Connor, M. B. (2015). Vesicle-mediated steroid hormone secretion in Drosophila melanogaster. *Cell.* **163**, 907-919. doi:10.1016/j.cell.2015.10.022

Yamauchi, T., Oi, A., Kosakamoto, H., Akuzawa-Tokita, Y., Murakami, T., Mori, H., Miura, M. and Obata, F. (2020). Gut bacterial species distinctively impact host purine metabolites during aging in Drosophila. *iScience* **23**, 101477. doi:10.1016/j.isci.2020.101477

Zinke, I., Schütz, C. S., Katzenberger, J. D., Bauer, M. and Pankratz, M. J. (2002). Nutrient control of gene expression in Drosophila: Microarray analysis of starvation and sugar-dependent response. *EMBO J.* **21**, 6162-6173. doi:10.1093/emboj/cdf600

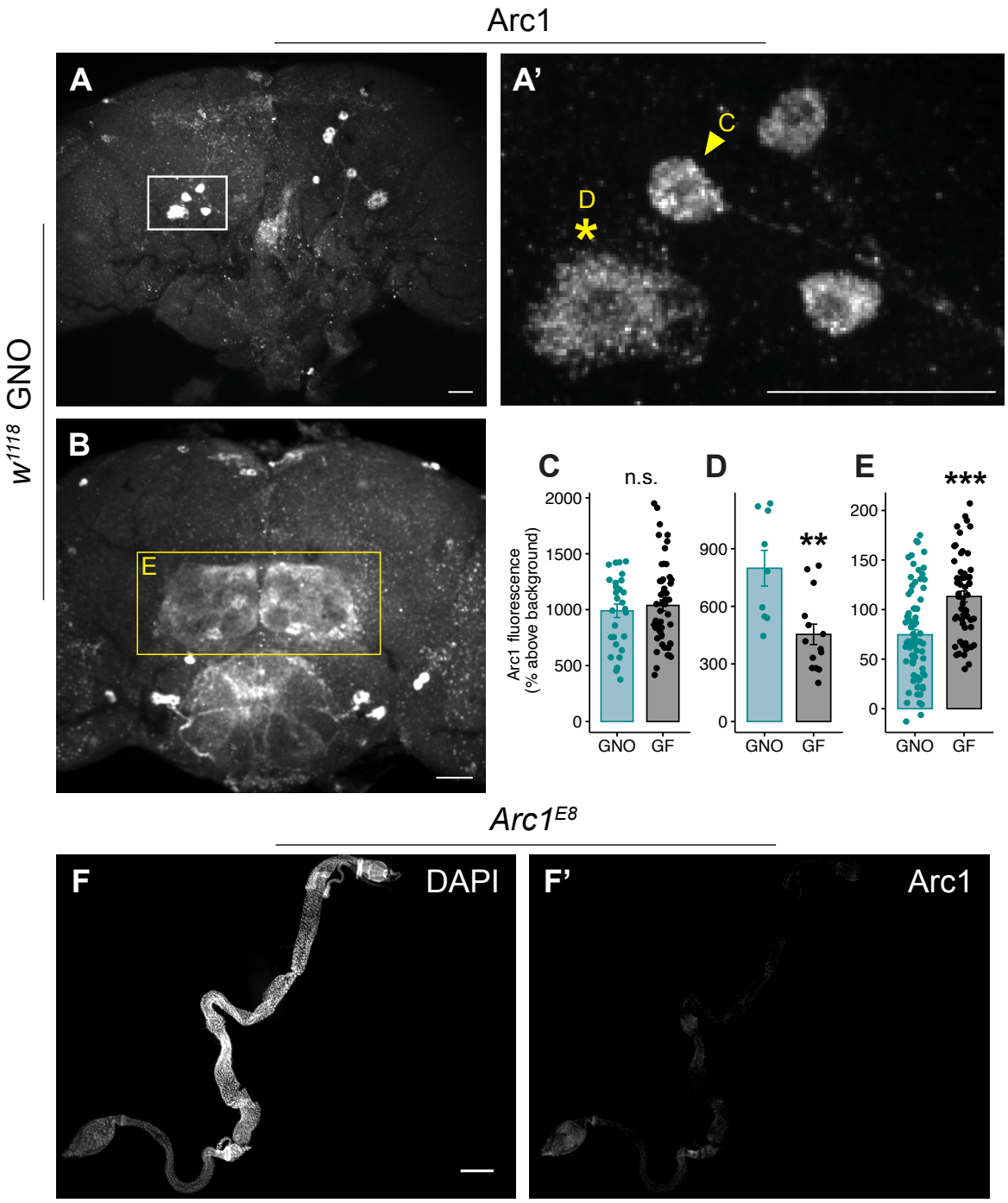

Fig. S1. Arc1 immunofluorescence in adult tissues. A,A'. Populations of Arc1-positive central brain cells with distinct Arc1 staining patterns in the posterior adult brain. **A'.** Higher magnification image of boxed region in **A**, showing clusters of central brain

neurons with concentrated bright Arc1 staining (example cell indicated with arrowhead), and nearby cells with weaker, more diffuse Arc1 staining (indicated with asterisk). **B.** Arc1 expression pattern on the anterior surface of adult brains. Boxed area indicates the antennal lobes. Scale bars: 5 μm (**A,A',B**). **C-E.** Arc1 fluorescence intensity comparisons between GNO and GF animals for different brain cell types. **C.** Arc1 intensity in brightly-labeled central neurons of the posterior brain (indicated with arrowhead in **A'**) is the same in GNO and GF flies. **D.** In GF animals, there is reduced signal in cells showing more diffuse Arc1 staining in the posterior adult brain (indicated with asterisk in **A'**). **E.** Increased Arc1 fluorescence intensity in the antennal lobes (boxed region in **B**) in GF *vs.* GNO brains. All analyses were conducted with 5-6 day old adult male w^{1118} flies. Individual points represent individual cells analyzed, **C,D** n=6-9 animals per condition. **E** n=7-8 animals per condition. **p<0.01, ***p<0.0001 n.s.=not significant, Mann-Whitney test (**C**) or Student's t-test (**D,E**). Error bars = s.e.m. **F,F'.** Arc1 staining in adult gut of *Arc1* null flies, showing minimal non-specific background staining. Scale bar: 200 μm.

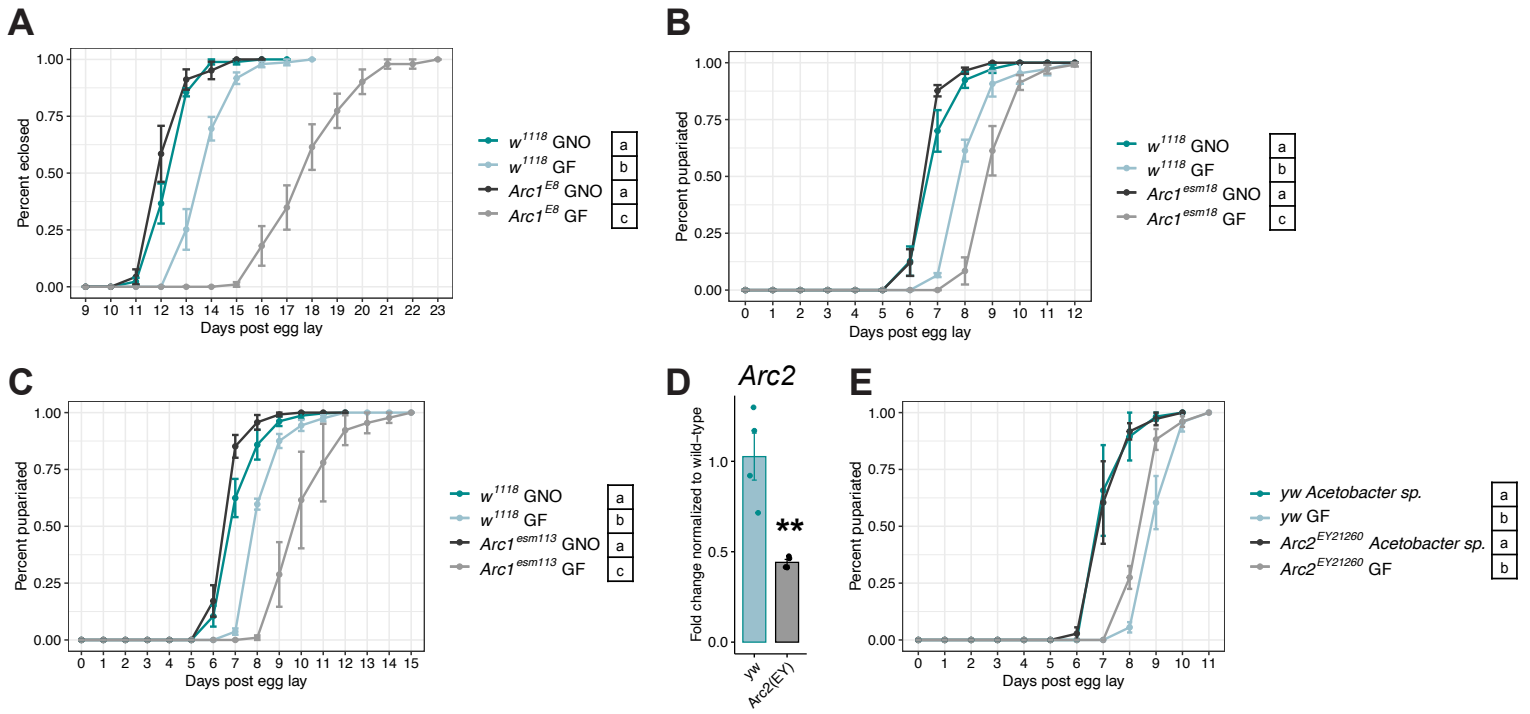

Fig. S2. Additional *Arc1* mutants are developmentally delayed under GF but not GNO conditions. A. Time to eclosion of wild-type and *Arc1* mutant populations represented in Fig. 2A. **B,C.** Time to pupariation for wild-type larvae and animals bearing independent *Arc1* mutant alleles. **D.** RT-qPCR of *Arc2* transcripts in whole pre-wandering third instar larvae of the indicated genotypes. $Arc2^{EY}$ is a random P-element insertion of $w^{+mC}y^{+mDint2}UASp$ in the 3' UTR of *Arc2*. Individual points represent normalized values for each biological replicate, 10 larvae per replicate. ** $p<0.01$, Student's t-test. **E.** Time to pupariation for wild-type and $Arc2^{EY}$ animals grown GF or in mono-association with *Acetobacter sp.* Reduction of *Arc2* does not impact time to pupariation. Error bars=s.e.m. For all developmental rate data **(A-C, E)**, conditions sharing a letter are not statistically different from one another, two-way ANOVA with Tukey's post-hoc test.

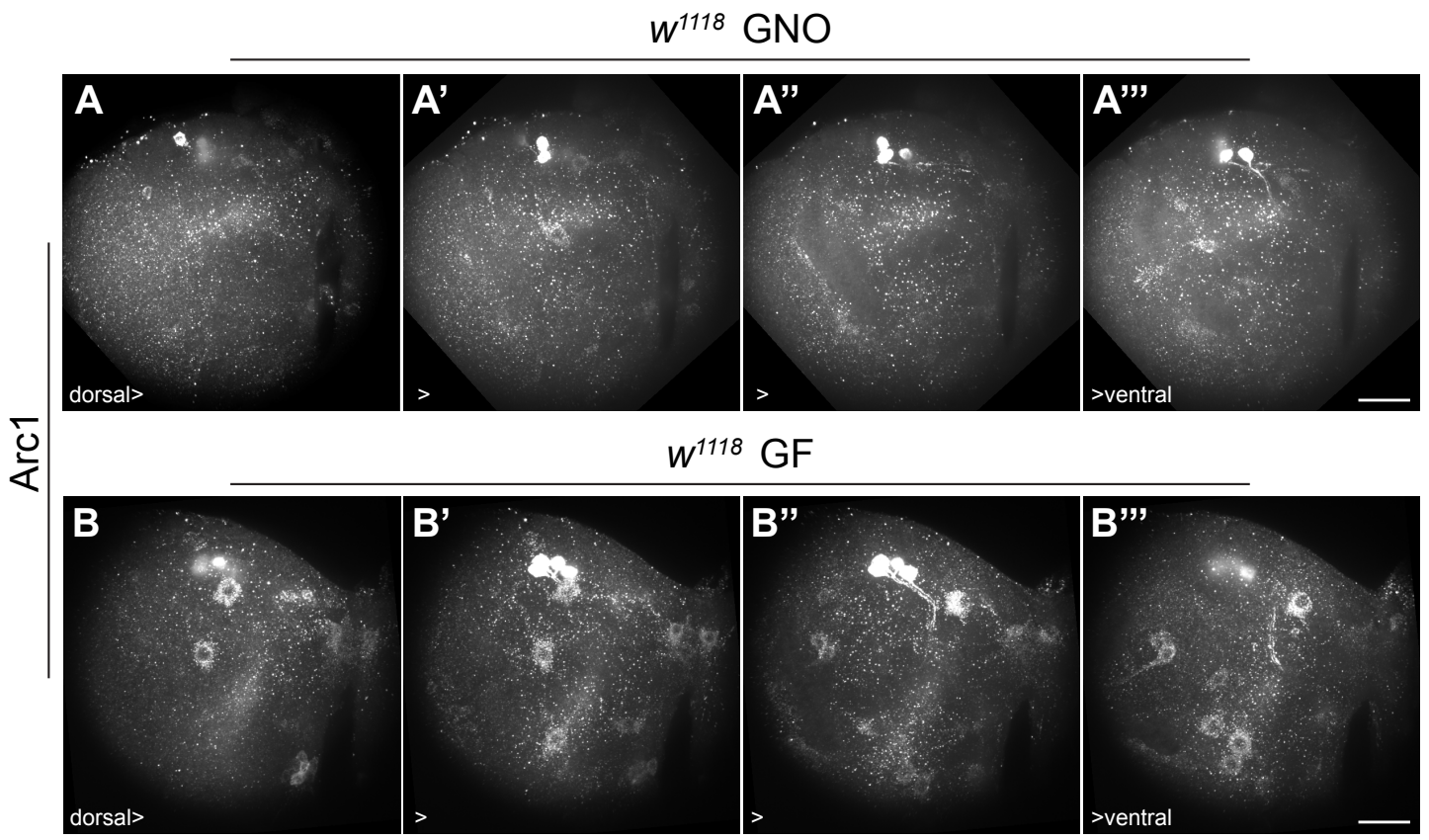

Fig. S3. Increased number of Arc1-positive cells in brains of GF larvae compared to GNO larvae. Arc1 staining in a representative lobe from each brain shown in Fig. 2D. Each image is a projection of eleven 0.2 µm slices. These are serial sections where the dorsal most sections are on the left and the ventral most sections are on the right. The signal is saturated in the highly expressing central brain neurons to more easily detect the other Arc1-positive cells that express at lower levels. Scale bar: 5 µm.

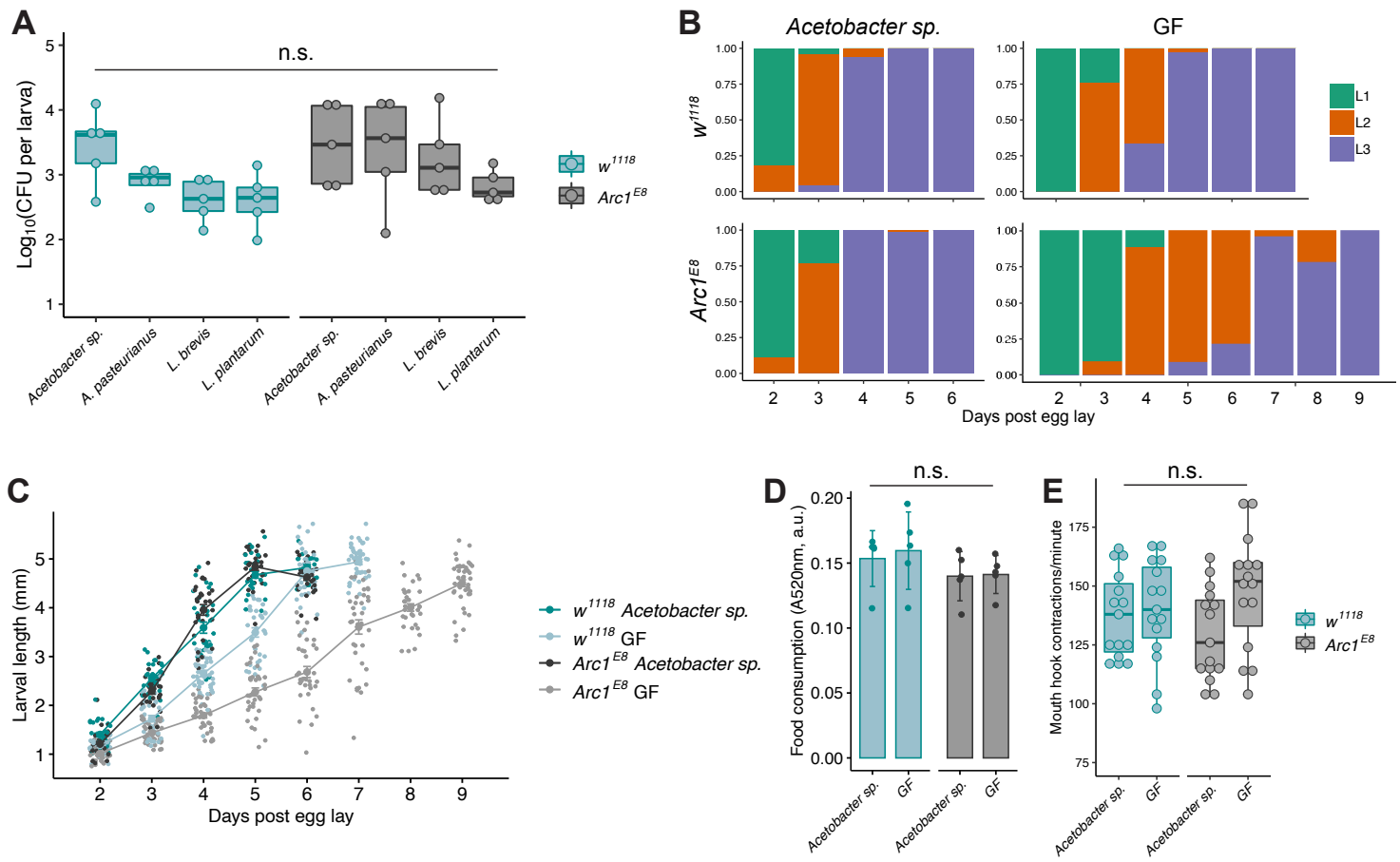

Fig. S4. Characterization of microbial loads, larval growth, and feeding behavior. A. Microbial loads for wild-type and *Arc1* mutant larvae mono-associated with the four bacterial isolates. Each data point represents a biological replicate of log-transformed colony forming unit (CFU) counts per larva recovered from surface-sterilized pre-wandering third instar larvae, 8-10 larvae per replicate. n.s.=not significant, two-way ANOVA with Tukey's post-hoc test. **B.** Percentage of larvae in the indicated instar stage daily until 100% of the population reaches the third instar stage. Data represent pooled percentages from three biological replicates for each day, ~30-60 animals per day. **C.** Larval length for both genotypes and microbial conditions over time. Each data point represents an individual larva, three biological replicates, ~10-20 larvae per replicate. **D.** Food consumed by larvae of each genotype and microbial condition in 30 min. Each data point represents food content in pooled guts of 20 pre-wandering third instar larvae. **E.** Mouth hook contraction rates, each point represents an individual larva. Error bars=s.e.m. n.s.=not significant, two-way ANOVA.

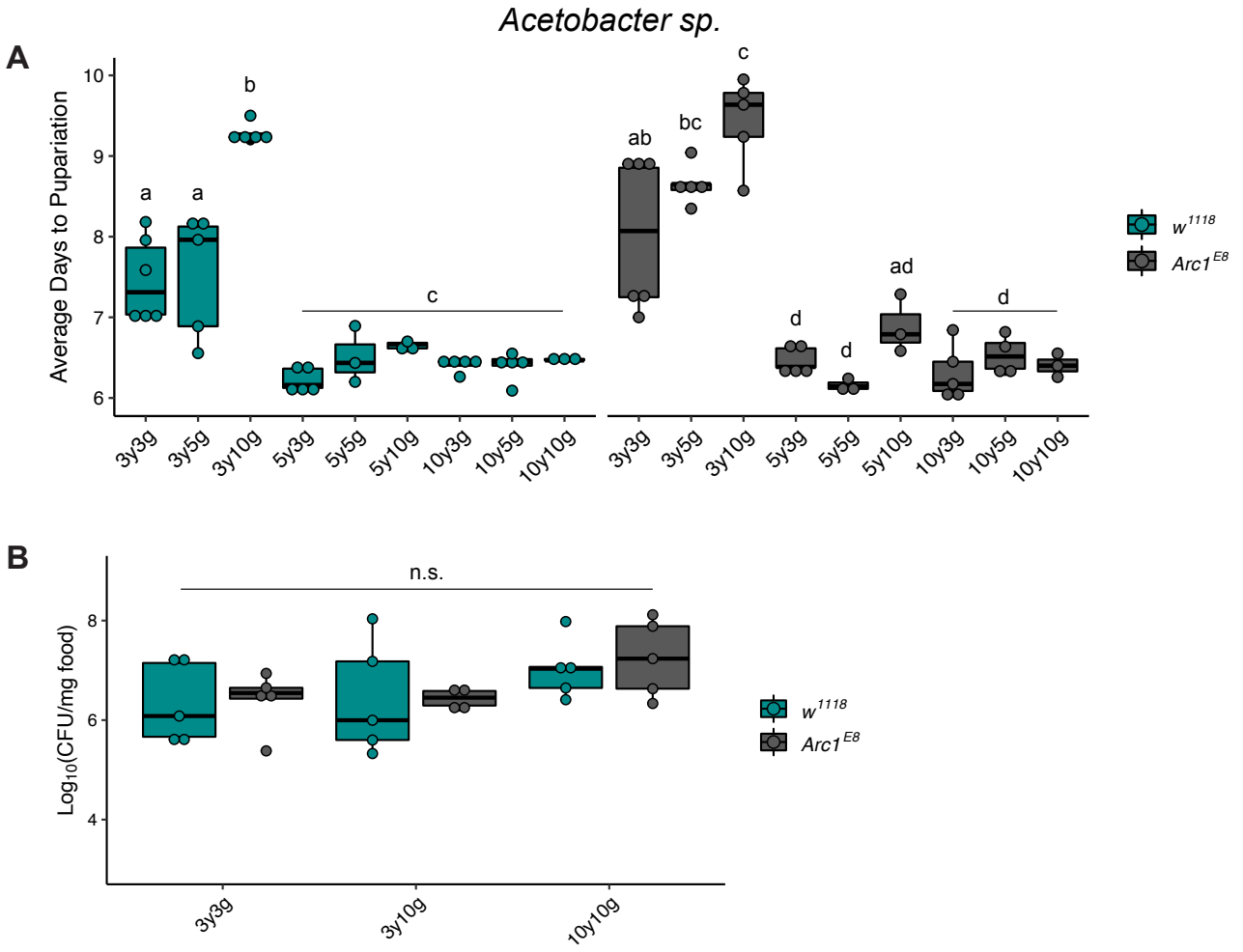

Fig. S5. *Acetobacter sp.* colonization of yeast-glucose diets. Testing the hypothesis that differences in *Acetobacter sp.*-associated larval growth rates among the various yeast-glucose diets **(A)** might result from varied *Acetobacter sp.*-colonization levels on these diets **(B)**. **A.** Developmental rate data for *Acetobacter sp.*-associated wild-type and *Arc1* mutant larvae grown on nine yeast-glucose diets. These are the same data presented in Fig. 3, but plotted collectively here for direct comparison of diet-dependent impacts on growth rate under *Acetobacter sp.*-associated conditions. **B.** *Acetobacter sp.* colonization levels on indicated diets. These three diets result in different growth rates for both genotypes, as shown in **A**., but *Acetobacter sp.* does not have significantly different levels of colonization on these diets. Conditions sharing a letter are not statistically different from one another, n.s.=not significant, each genotype compared by one-way ANOVA with Tukey's post-hoc test.

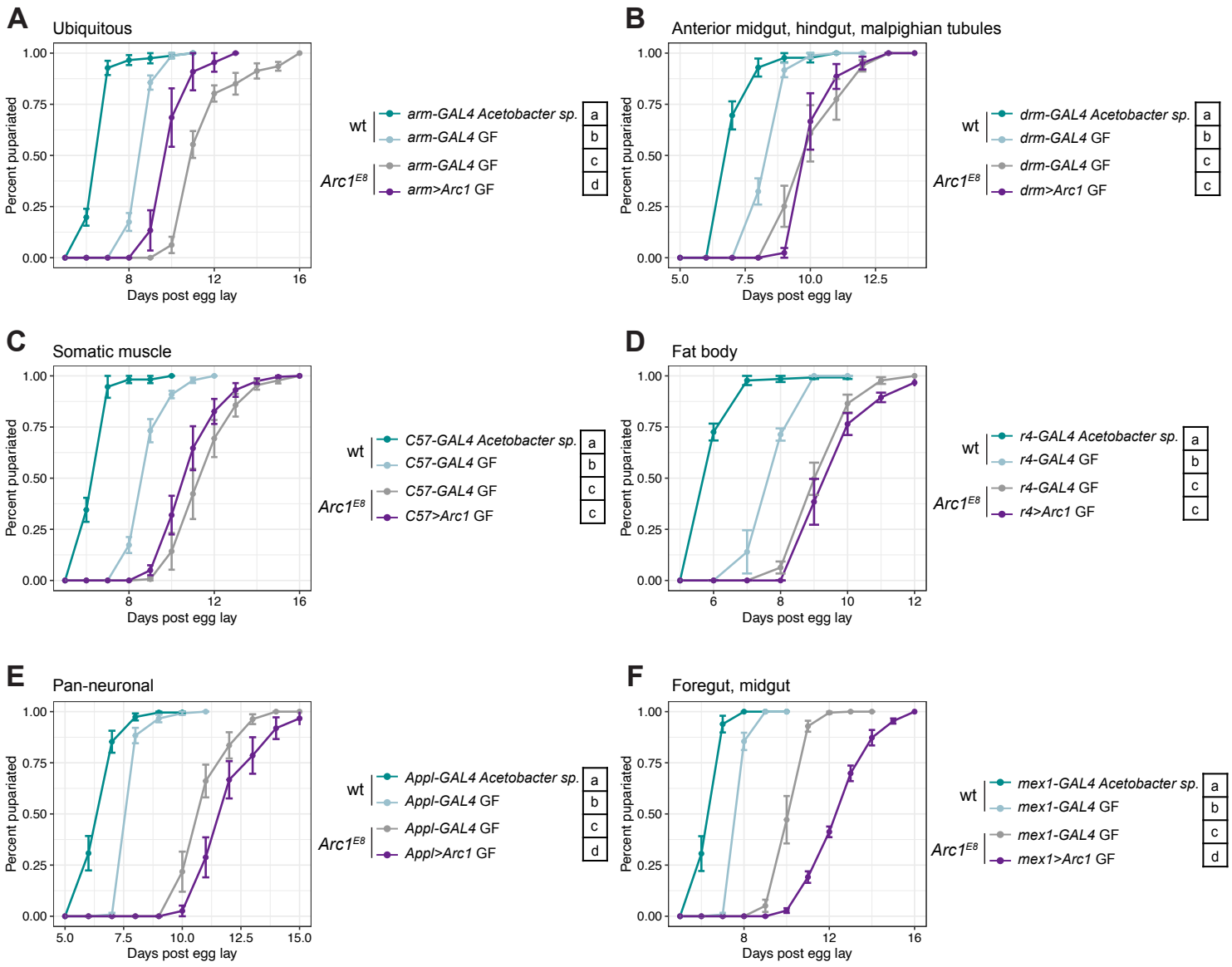

Fig. S6. Tissue-specific Arc1 rescue under GF conditions. Time to pupariation for GF *Arc1*^{E8} animals in which Arc1 expression has been restored via the indicated tissue- and cell-type-specific GAL4 drivers. *Arc1*^{E8}*;GAL4* GF controls and *Arc1*^{E8}*;GAL4>Arc1* GF data are same as presented in Fig. 6A, but full growth curves are depicted here, along with *Acetobacter sp.*-associated and GF wild-type *GAL4* controls for reference. Control animals (*GAL4* alone in wild-type and *Arc1*^{E8} backgrounds) are heterozygous for the *GAL4* transgene. Conditions sharing a letter are not statistically different from one another, one-way ANOVA with Tukey's post-hoc test.

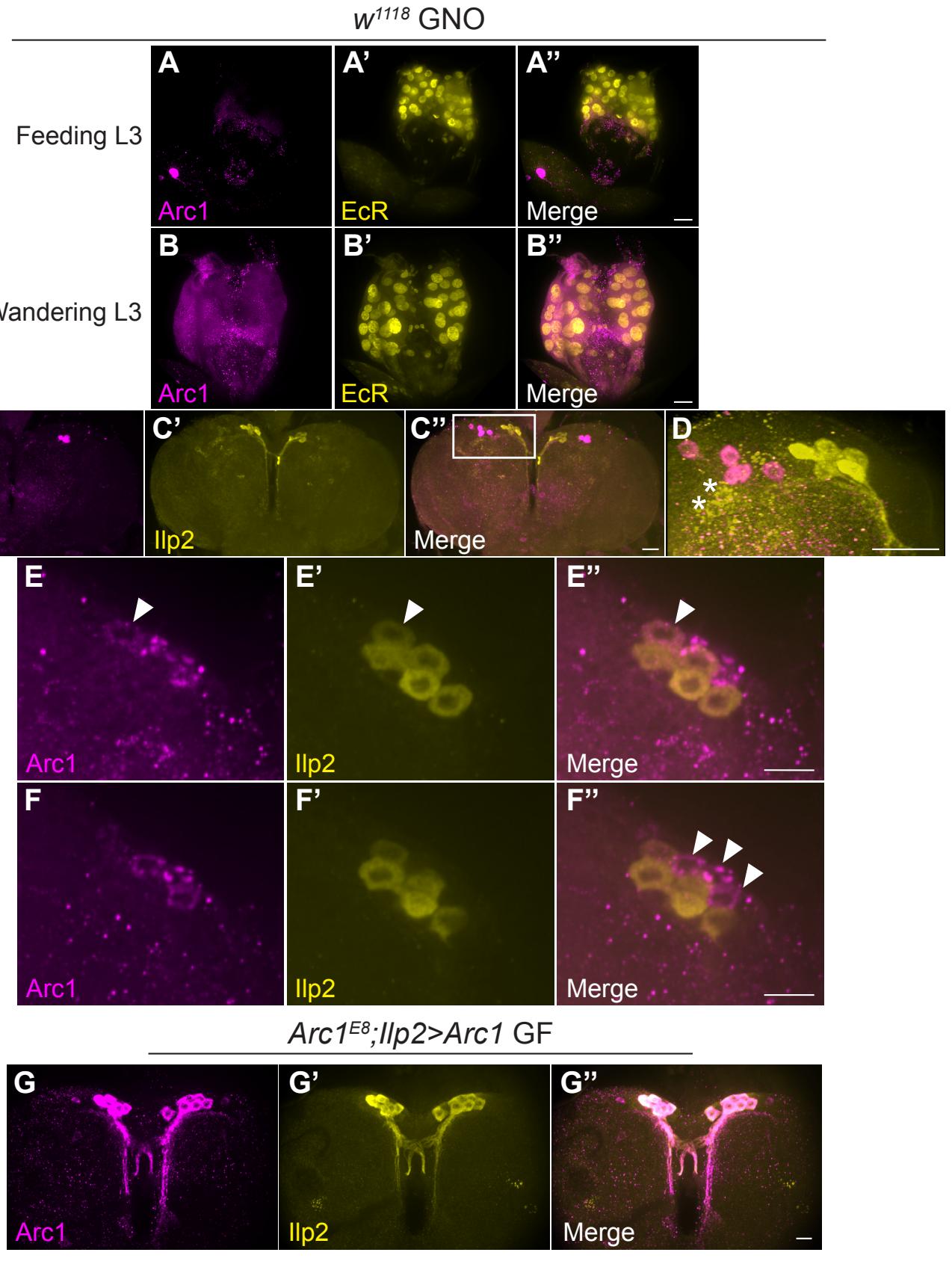

Fig. S7. Wild-type Arc1 expression patterns in the ring gland and IPCs. A-B''. Arc1 immunostaining level in the ring gland increases between the feeding and wandering third larval instar (L3) stages. Images were acquired with the same laser power and exposure and adjusted identically in Adobe Photoshop. Ring gland nuclei are labelled with anti-ecdysone receptor (EcR). Scale bar: 5 μm. **C-D.** Arc1-positive cells in the central larval brain shown in relation to the IPCs (labelled with anti-Ilp2). **D.** Boxed region in **C''** is shown at higher magnification in **D**. Image in **D** is from a rotated 3D projection of 125 0.2 μm slices. Two Ilp2-positive cells outside the IPC cluster and adjacent to the Arc1-positive cluster are indicated (asterisk). Scale bar: 5 μm **(C-C'')** and 5 μm **(D)**. **E-F''.** Projections of six 0.2 μm slices from two different focal planes of the same IPC cluster. Some IPCs exhibit weak Arc1 labelling (example indicated with arrowhead **E-E''**). We also observed Arc1-positive, Ilp2-negative cells adjacent to the Ilp2-positive cluster (arrowheads **F-F''**). Scale bar: 5 μm. **G-G''.** Strong, ectopic Arc1 expression in the IPCs in *Arc1^{E8};Ilp2>Arc1* rescue animals (compare to Fig. 2D and S7C-F''). Scale bar: 5 μm.

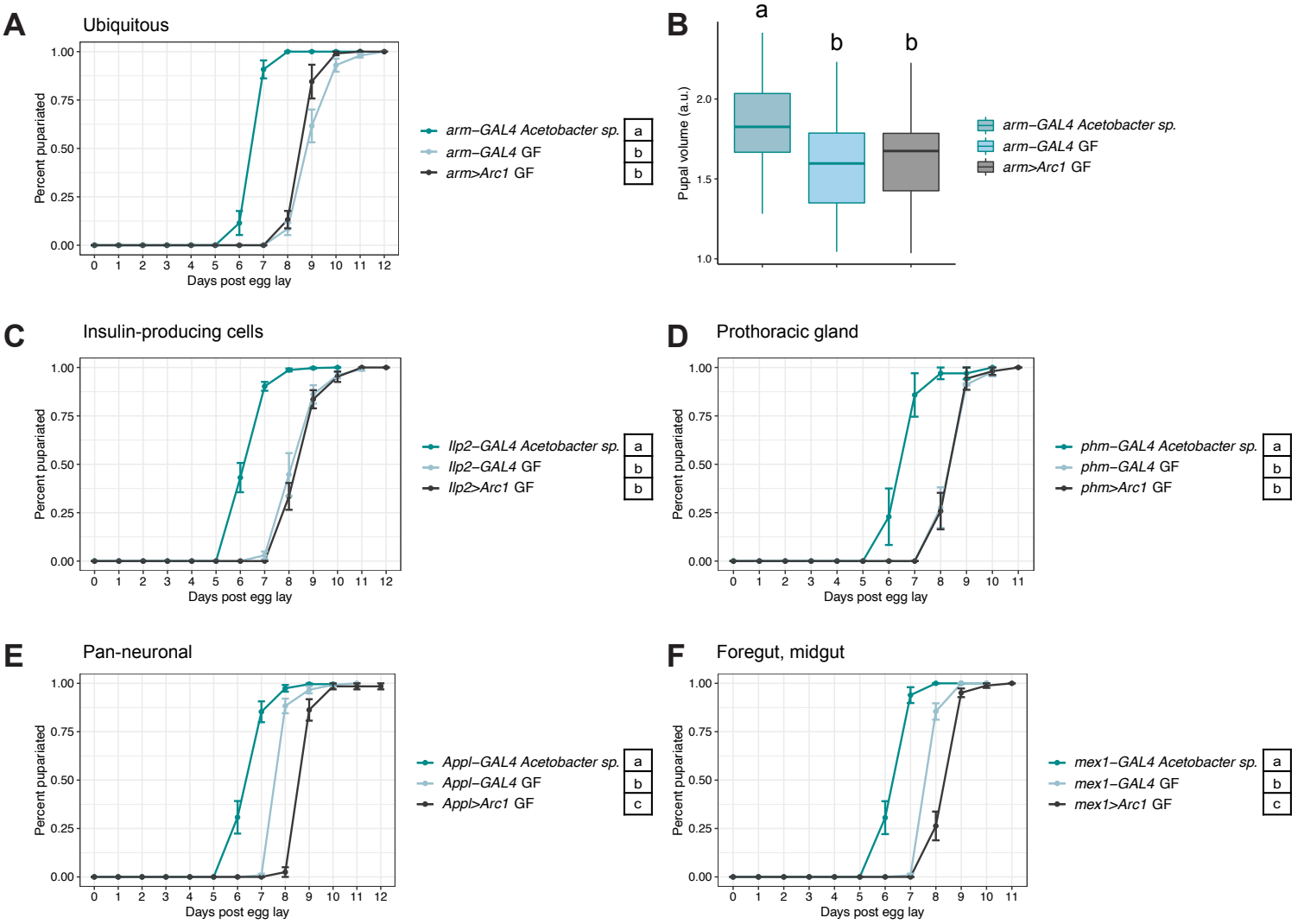

Fig. S8. Effects of Arc1 overexpression in wild-type GF larvae on growth rate and pupal size. A, B. Weak ubiquitous overexpression of Arc1 does not impact time to pupariation or pupal volume under GF conditions. For **B** n=37-54 pupae per condition. **C-F.** Pan-neuronal and midgut enterocyte-specific, but not IPC- or prothoracic gland-specific Arc1 overexpression delays development in GF wild-type animals. Developmental rate data for *GAL4* control animals (except GF *arm-GAL4*) are the same as in Fig. 6B,C and S6A-C, presented again here for direct comparison to overexpression animals. Conditions sharing a letter are not statistically different from one another, one-way ANOVA with Tukey's post-hoc test.

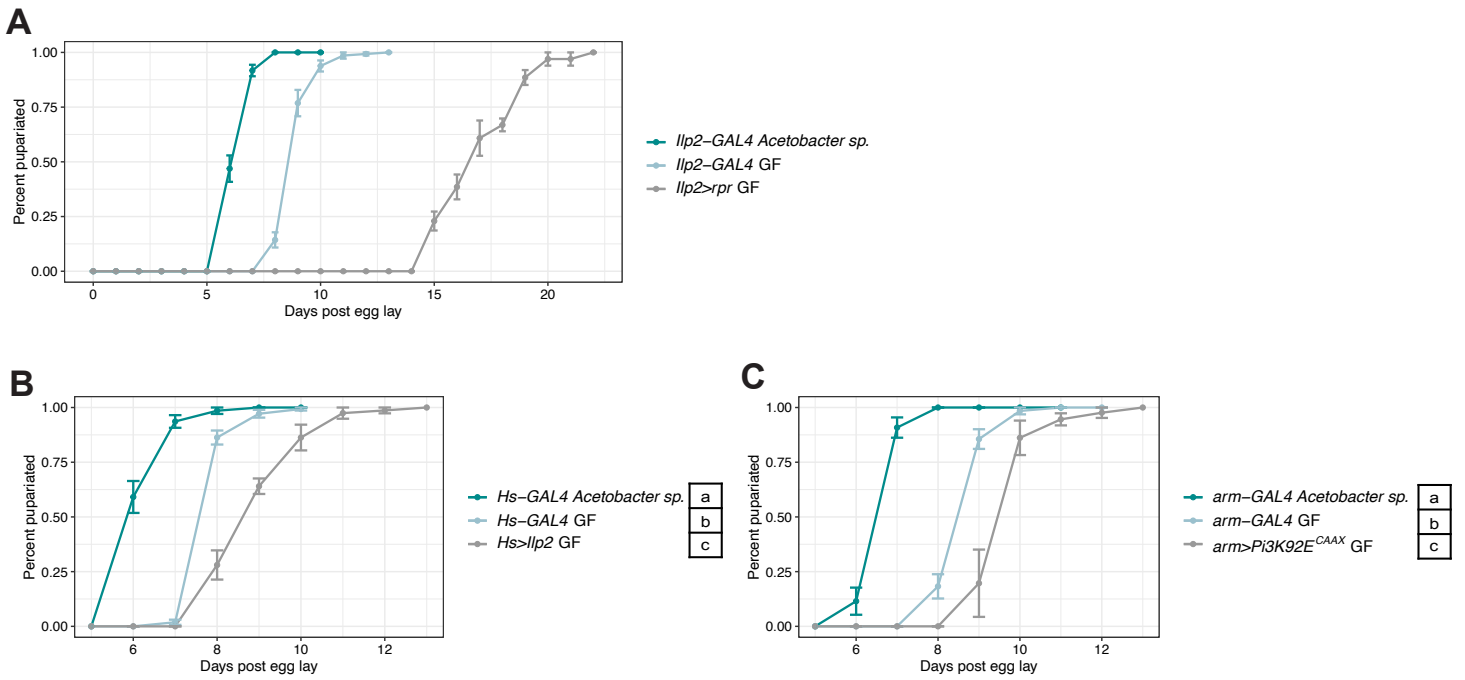

Fig. S9. Systemic over-activation of insulin signaling or ablation of the IPCs in GF larvae induces developmental delay. A. Expressing the pro-apoptotic *reaper* in IPCs causes severe developmental delay in GF larvae as previously shown (Rulifson et al., 2002). **B,C.** Reduced growth rate in GF larvae following IIS pathway activation via periodic heat shock-induced ubiquitous expression of Ilp2 (**B**; Brogiolo et al., 2001) or weak ubiquitous expression of membrane-targeted, constitutively active Pi3K (**C**; Homem et al., 2014). In **A** and **C**, developmental rate data for *GAL4* control animals (except GF *Ilp2-GAL4*) are same as presented in Fig. S6A and Fig. 6C, shown again here for reference. Conditions sharing a letter are not statistically different from one another, one-way ANOVA with Tukey's post-hoc test.

Table S1. Sample sizes, summary statistics, and test results for developmental rate experiments

Click here to download Table S1

Table S2. Primers used for RT-qPCR analysis

Gene	Forward (5'-3')	Reverse (5'-3')	Reference
Rpl32	ATGCTAAGCTGTCGCACAAATG	GTTCGATCCGTAACCGATGT	Ponton et al., 2011
Arc1	CATCATCGAGCACAACAACC	CTACTCCTCGTGCTGCTCCT	Mosher et al., 2015
Arc2	CGTGGAGACGTATAAAGAGGTGG	GACCAGGTCTTGGCATCCC	FlyPrimerBank; Hu et al., 2013
Thor/4EBP	CAGATGCCCGAGGTGTACTC	CATGAAAGCCCGCTCGTAGA	
InR	AACAGTGGCGGATTCGGTT	TACTCGGAGCATTGGAGGCAT	Obata et al., 2018
Ilp2	GTATGGTGTGCGAGGAGTAT	TGAGTACACCCCCAAGATAG	Shin et al., 2011
Ilp3	AAGCTCTGTGTGTATGGCTT	AGCACAATATCTCAGCACCT	
Ilp5	AGTTCTCCTGTTCCTGATCC	CAGTGAGTTCATGTGGTGAG	
spok	TATCTCTTGGGCACACTCGCTG	GCCGAGCTAAATTTCTCCGCTT	Christensen et al., 2020
sro	CGAATCGCTGCACATGAC	TAGGCCCTGCAGCAGTTTAG	Ou et al., 2016
nvd	GGAAGCGTTGCTGACGACTGTG	TAAAGCCGTCCACTTCCTGCGA	Pankotai et al., 2010
phm	GGATTTCTTTCGGCGCGATGTG	TGCCTCAGTATCGAAAAGCCGT	
dib	TGCCCTCAATCCCTATCTGGTC	ACAGGGTCTTCACACCCATCTC	
sad	CCGCATTCAGCAGTCAGTGG	ACCTGCCGTGTACAAGGAGAG	
shd	CGGGCTACTCGCTTAATGCAG	AGCAGCACCACCTCCATTTC	

References

Christensen, C. F., Koyama, T., Nagy, S., Danielsen, E. T., Texada, M. J., Halberg, K. A. and Rewitz, K. (2020). Ecdysone-dependent feedback regulation of prothoracicotropic hormone controls the timing of developmental maturation. *Dev.* **147**, dev188110.

Homem, C. C. F., Steinmann, V., Burkard, T. R., Jais, A., Esterbauer, H. and Knoblich, J. A. (2014). Ecdysone and mediator change energy metabolism to terminate proliferation in drosophila neural stem cells. *Cell* **158**, 874–888.

Hu, Y., Sopko, R., Foos, M., Kelley, C., Flockhart, I., Ammeux, N., Wang, X., Perkins, L., Perrimon, N. and Mohr, S. E. (2013). FlyPrimerBank: an online database for Drosophila melanogaster gene expression analysis and knockdown evaluation of RNAi reagents. *G3, Genes, Genomes, Genet.* **3**, 1607-1616.

Obata, F., Fons, C. O. and Gould, A. P. (2018). Early-life exposure to low-dose oxidants can increase longevity via microbiome remodelling in Drosophila. *Nat. Commun.* **9**, 975.

Ou, Q., Zeng, J., Yamanaka, N., Brakken-Thal, C., O'Connor, M. B. and King-Jones, K. (2016). The Insect Prothoracic Gland as a Model for Steroid Hormone Biosynthesis and Regulation. *Cell Rep.* **16**, 247–262.

Pankotai, T., Popescu, C., Martín, D., Grau, B., Zsindely, N., Bodai, L., Tora, L., Ferrús, A. and Boros, I. (2010). Genes of the Ecdysone Biosynthesis Pathway Are Regulated by the dATAC Histone Acetyltransferase Complex in Drosophila. *Mol. Cell. Biol.* **30**, 4254–4266.

Ponton, F., Chapuis, M. P., Pernice, M., Sword, G. A. and Simpson, S. J. (2011). Evaluation of potential reference genes for reverse transcription-qPCR studies of physiological responses in Drosophila melanogaster. *J. Insect Physiol.* **57**, 840–850.